UQAC
Université du Québec
à Chicoutimi

DECODING THE SEASONAL CLOCK OF SUGAR MAPLE: TIMINGS AND SEQUENCE OF ITS PHENOLOGICAL EVENTS

par Rachana Bhandari

Mémoire présenté à l'Université du Québec à Chicoutimi en vue de l'obtention du grade de Maîtrise ès sciences (M. Sc.) en ressources renouvelables.

Québec, Canada

RÉSUMÉ

Le calendrier saisonnier des processus physiologiques chez l'érable est essentielle pour comprendre les stratégies d'allocation saisonnière du carbone et la dynamique de la production de sève. Chez l'érable à sucre (Acer saccharum), ces processus déterminent le moment et l'efficacité de la production de sève ainsi que la croissance globale de l'arbre. Comprendre la succession de ces événements et identifier des méthodes fiables pour les suivre est donc fondamental tant pour l'avancement des connaissances écologiques que pour les études phénologiques. Cette mémoire porte sur la phénologie de l'érable à sucre à travers deux études complémentaires. La première étude a examiné la séquence et l'ordre chronologique des différents événements phénologiques chez l'érable à sucre à Simoncouche, Québec, Canada, sur une période de cinq ans (2018-2022). Le suivi de la saison des sucres, du transport de l'eau et de la croissance radiale a été réalisé à l'aide de pluviomètres et de dendromètres automatiques installés sur quatre érables à sucre matures et dominants. Pour étudier la phénologie foliaire (débourrement, feuillaison et chute des feuilles), nous avons utilisé l'indice de végétation par différence normalisée (NDVI) dérivé de MODIS dans quatre érablières situées à proximité du site d'étude. Dans cette région, la saison des sucres commençait à la fin mars et se terminait au début mai, coïncidant avec la fonte des neiges et l'augmentation de l'humidité du sol. De plus, la fin de la saison des sucres coïncidait avec le début du transport de l'eau par tension. Le débourrement survenait une semaine après le début de ce transport de l'eau. La feuillaison avait lieu trois semaines après, vers la mi-mai. Deux semaines plus tard, au début de juin, commençait la croissance radiale, qui se poursuivait jusqu'au début août. La fin du transport de l'eau par tension entraînait la chute des feuilles au début de novembre. En 2021, année caractérisée par un printemps chaud, nous avons observé un avancement d'au moins trois semaines de l'ensemble des événements phénologiques étudiés. En mettant l'accent sur la nature séquentielle des événements phénologiques et leurs relations physiologiques, cette étude contribue à une meilleure compréhension de la phénologie végétale et de la dynamique du carbone. Les résultats offrent également des pistes pratiques pour l'industrie acéricole, soulignant l'importance du suivi des signaux environnementaux afin d'optimiser les stratégies d'entaillage dans un contexte de changements climatiques. Le deuxième chapitre a évalué la fiabilité des indices dérivés des phénocams pour le suivi de la phénologie automnale. À l'aide d'images à haute fréquence recueillies à L'Assomption, Québec, durant l'automne 2023, trois indices ; la coordonnée chromatique verte (GCC), la coordonnée chromatique rouge (RCC) et l'indice de vert excédentaire (ExG) ont été comparés aux observations de terrain. La GCC et l'ExG ont le mieux capturé le début du changement de couleur des feuilles, tandis que la RCC prédisait le plus fidèlement le moment de la chute des feuilles. Ces résultats démontrent que les phénocams constituent un outil rentable et complémentaire aux observations de terrain, notamment dans les situations où un suivi continu est difficile à réaliser.

Mots-clés : *Acer saccharum,* phénologie, saison des sucres, croissance radiale, feuillaison, transport de l'eau

ABSTRACT

The seasonal calendar of the physiological processes in maple is essential to understand the strategies of seasonal carbon allocation and the dynamics of sap production. In sugar maple (*Acer saccharum*), these processes determine the timing and efficiency of sap production as well as overall tree growth. Understanding the sequence of these events and identifying reliable methods to monitor them are therefore essential for advancing both ecological knowledge and phenological studies. This thesis studies sugar maple phenology through two complementary studies. The first study examined the sequence and chronological order of different phenological events in sugar maple in Simoncouche, Quebec, Canada over a period of five years (2018-2022). The timing of sugar season, water transport and radial growth was accessed using rain gauges and automatic point dendrometers installed in four mature and dominant sugar maple trees. To study the timing of leaf phenology (budburst, leafing and leaf fall), we relied on MODIS-derived Normalized Difference Vegetation Index (NDVI) in four maple stands near the study area. In the study area, the sugar season began in late March and ended in early May, coinciding with snowmelt and increasing soil moisture. Furthermore, the end of sugar season coincided with the onset of tension driven water transport. Budbreak occurred one week after the onset of tension driven water transport. Leafing occurred three weeks after the onset of tension driven water transport around mid-May. Two weeks after the leafing in early June, the radial growth started in maples which continued until early August. The end of tension-driven water transport led to leaf fall in early November. In 2021, which had a warm spring, we observed the earlier onset of the studied phenological events by at least three weeks. By emphasizing the sequential nature of phenological events and their physiological relationships, this study contributes to a broader understanding of plant phenology and carbon dynamics. The results also offer practical insights for the maple syrup industry, emphasizing the importance of monitoring environmental signals to optimize tapping strategies under changing climatic conditions. The second chapter evaluated the reliability of phenocam-derived indices for monitoring autumn phenology. Using high-frequency images collected in L'assomption, Quebec during autumn 2023, three indices; green chromatic coordinate (GCC), red chromatic coordinate (RCC), and excess green index (ExG) were compared with field observations. GCC and ExG best captured the onset of leaf color change, whereas RCC best predicted the timing of leaf fall. These results demonstrate that phenocams provide a cost-effective and alternative tool to field-based observations, particularly in situations where continuous monitoring is challenging.

Keywords: *Acer saccharum*, phenology, sugar season, radial growth, leafing, water transport

Table of Contents

List of Tables

List of Figures

ACKNOWLEDGEMENTS

I would like to begin by expressing my sincere gratitude to my director Professor Sergio Rossi for his constant guidance, encouragement, support and supervision throughout my masters. Nothing would have been possible without his support. His availability to answer my doubts and solve any problems helped me in taking this project forward. Thank you for believing in me and providing me this interesting project for my research.

I would like to mention my gratitude to Dr. Roberto Silvestro for his support and guidance throughout my research duration. Next, I am thankful towards my lab group for creating a productive and enjoyable environment to work with. I would like to say special thanks to Sara for her support during the data collection before the start of the masters. Special thanks to my partner, Bijay for his constant support and encouragement throughout my study. I appreciate the love and support of all my friends here in Chicoutimi during this journey.

I would like to thank my family and friends back home for their support. The love and support from my family have always motivated me to work and progress more.

GENERAL INTRODUCTION

Maple syrup production has been holding a long symbolic place in the history of Canada since the 18th and 19th century. Apart from its cultural significance, maple syrup has high economic value, making it a major contributor in Canadian economy. The gross value of Canadian maple syrup reached $837.3 million in 2024, an increase of nearly 49% since 2020. The export of Canadian maple products rose by 16% from 2023, reaching $715.9 million and exporting to 71 different countries (Agriculture and Agri-Food Canada 2025). The maple syrup industry generates the tax revenues of $235 million to the government of Quebec and the rest of Canada. In 2025, Quebec recorded a total of 225 million pounds of maple syrup with an average yield of 4.04 pounds per tap (Agriculture and Agri-Food Canada 2025). The maple syrup industry has created approximately 12,600 full time job opportunities across the region.

There are more than 150 species of maple globally while only about a dozen of them are found in North America. Among all these species, some commonly tapped maple species are sugar maple (*Acer saccharum* Marsh.*),* red maple *(Acer rubrum* L.*),* black maple *(Acer nigrum* F. Michx.*)* and silver maple *(Acer saccharinum* L.*)* (Ramadan et al. 2021). Among these species, sugar maple is commonly tapped due to its high sugar concentration in the sap. Sugar maple is distributed along northeastern United States to southeastern regions of Canada (Boakye et al. 2023). The species grow in cool and moist climates and are mostly found in mixed forests along with other temperate broadleaf species. Like many other tree species, sugar maple also poses various stages from sugar season in spring to leaf fall in autumn

and dormancy during winter. These events have their own physiological process that guide the tree functioning and vitality across the annual cycle.

Plant phenology is the study of timing of different life cycle events in plants starting from spring greenness proceeding to summer maturity, autumn senescence, and suspending the usual activities with winter dormancy (Zhang *et al.* 2003). In winter, plants enter dormancy where they suspend or slow down their usual activities to protect vulnerable tissues from harsh winter conditions. During late winter and early spring, maple sap is collected from the mature sugar maple trees by making a taphole in the tree. Maple sap usually exudates in the presence of freeze thaw cycles when the nighttime temperatures reach below zero and the daytime temperatures exceed the freezing point. These alternating temperatures create positive pressure in the xylem of the tree which leads the sap to come out from the tapholes (Graf et al. 2015). With the rise in temperatures and the ending of freeze thaw cycles to generate positive pressure in the tree, the sap season gradually ends, and the tree marks the shift to physiologically active phase (Perkins et al. 2022). During spring, budbreak is the first event to occur followed by the leafing, and secondary growth and eventual senescence and abscission of leaves. These events in the trees are related to each other. For instance, budbreak must occur on the trees for the leaves to come out and for the active photosynthesis to start in the trees (Ettinger 2018).

Climate change is becoming a global issue with pronounced effects on vegetation dynamics and plant physiology. This effect is also evident in maple syrup production with producers across different maple producing regions reporting noticeable changes in the timing and duration of the sugaring season with an

increased variability from year to year (Ahmed et al. 2023). Along with the effect on the maple sap production, climate change may also alter the overall phenological events of sugar maple with the warmer springs progressing the growing season (Guo et al. 2020). Such changes are closely tied to climatic drivers, especially temperature and snow dynamics, yet the relationship between sap flow timing and the broader sequence of sugar maple phenophases remains less explored. Understanding these relationship is critical, as shifts in phenological timing could affect not only maple syrup yields and forest productivity but also the ecological resilience of sugar maple stands under future climate conditions.

Phenology and its timing can be studied using different methods and tools. Traditional field observations are essential for accurately documenting phenological events, especially for canopy phenology (eg., budburst, leafing, leaf senescence and leaf fall). But these methods are time consuming, labor-intensive and limited on a spatial and temporal scale. To complement these methods, digital repeat photography using phenocams has emerged as a powerful tool for near-continuous monitoring of canopy dynamics. Digital cameras record high frequency images that can be transformed into greenness indices, making them useful for detecting key transitions in phenology (Richardson et al. 2018). Evaluating the accuracy of phenocam-derived metrics against detailed field observations is therefore essential for determining their potential as long-term monitoring tools.

To address the challenges, this thesis focuses on two aspects of sugar maple phenology. First, I examine the timings and sequence of multiple phenological events throughout the year for the period of five years (2018 to 2022) using mature and healthy sugar maple trees located in Chicoutimi, Quebec, Canada. To achieve

this, a combination of data sources was used such as rain gauge measurements, dendrometers, and remote sensing. I studied the events starting from the transition from dormancy to spring through the sugar season, budbreak, leafing, radial growth and ultimately to leaf fall. Secondly, I evaluated the reliability of phenocam-derived metrics compared with field observations, using one year of autumn data in the year 2023.

CHAPTER I

DECODING THE SEASONAL CLOCK OF SUGAR MAPLE: TIMINGS AND SEQUENCE OF ITS PHENOLOGICAL EVENTS

Published in: Trees Forests and People

Bhandari, R., Silvestro, R., & Rossi, S. (2025). Decoding the seasonal clock of sugar maple: timings and sequence of its phenological events. *Trees, Forests and People, 101020.*

Authors:

Rachana Bhandari[1*], Roberto Silvestro[1], Sergio Rossi[1]

Affiliations:

1 Laboratoire sur les écosystemes terrestres boreaux, Département des Sciences Fondamentales, Université du Québec à Chicoutimi, Chicoutimi, QC, Canada

*Corresponding author: rbhandari@etu.uqac.ca

1.1 Abstract

The seasonal sequence of physiological processes is essential to understand the strategies of carbon allocation and the dynamics of sap production in maple. We monitored the phenological events in sugar maple (Acer saccharum Marsh.) from 2018 to 2022 in Simoncouche (QC), Canada. We measured sap exudation, xylem water transport and radial growth using rain gauges and dendrometers installed on four adult trees. Leaf phenology was estimated with MODIS-derived Normalized Difference Vegetation Index (NDVI) in maple stands near the study site. The sugar season started in late March and ended in early May, at the onset of tension-driven water transport. The sugar season corresponded with the period of snowmelt and increase in soil water content. Budbreak and complete leaf expansion were observed one and two weeks after the ending of sap exudation, respectively, when the snow had disappeared and soil temperature started rising. Radial growth occurred two weeks after leaf expansion and ended in early August. The cessation of xylem water transport caused leaf fall in early November. Phenology advanced up to three weeks during the warm spring 2021. The synchronism between the sugar season and tension-driven water transport confirms the physiological limit for sap exudation, suggesting the importance of optimizing yield within the time window of rehydration after winter dormancy. In the context of ongoing climate warming, producers could benefit from paying more attention to the environmental and physiological signals triggering the sap season rather than relying solely on historical calendars of sap production.

Keywords: *Acer saccharum*, phenology, sugar season, radial growth, leafing, water transport

Graphical abstract

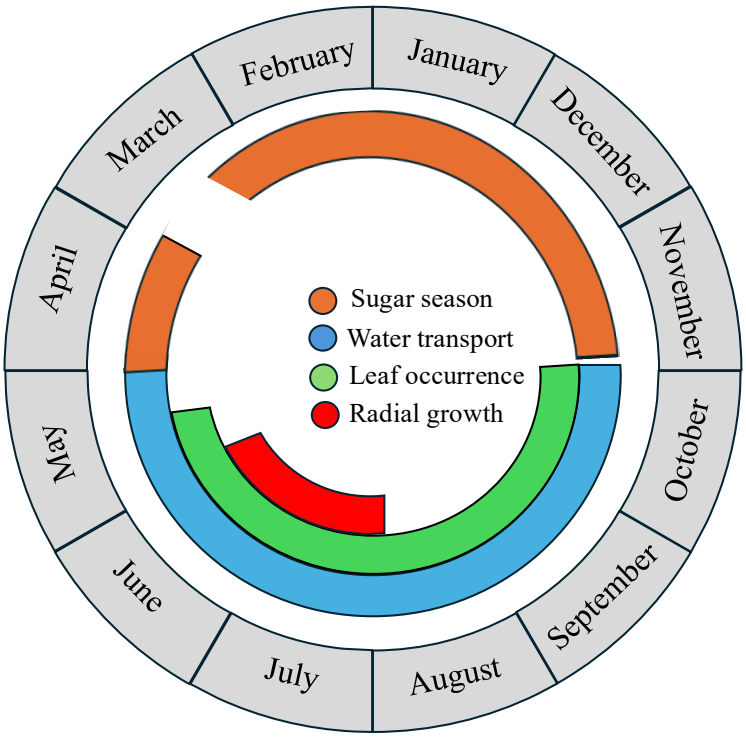

1.2 Introduction

Canada is the global leader in maple syrup production, accounting for approximately 73% of the world's supply, with over 90% of that production originating from Quebec alone (Agriculture and Agri-Food Canada 2025). The sap from which the syrup is obtained is harvested from mature sugar maple (*Acer saccharum* Marsh.) trees during late winter to early spring, a short and yet important time window in the annual cycle of the species (Kurokawa et al. 2022). However, increasing temperatures, shifting precipitation patterns and altered freeze-thaw cycles might increasingly affect maple physiology and, possibly, syrup yields (Rapp et al. 2019). While the sugar season draws considerable attention among researchers, it represents only one phase of a complex, interconnected sequence of events. Expanding our focus beyond the sugar season to understand the timing and coordination of multiple phenological stages throughout the year can provide critical insights to assess the biological processes underlying maple syrup production.

Plant phenology is the study of the timings of plant recurrent life-cycle events and their biotic and abiotic drivers (Gray et Ewers 2021). It determines the ability of plants to adapt to local climates, to compete for resources and avoid environmental stressors (Silvestro et al. 2025). Phenological stages are not isolated events but components of a sequential chain, where the timing of one stage often affects the start and length of the next one (Rossi et al. 2012). The temporal sequence of phenological events plays a major role in regulating the ecosystem processes, such as carbon allocation and sequestration (Silvestro et al. 2024). However, the considerable variation in phenological responses across species and years shows

that the mechanisms governing these processes are complicated, involving both external climatic signals and internal physiological controls (Park et Post 2022). Sugar maple, a species of ecological and economic importance in North American forestry and agriculture industries, offers a great model for studying how trees coordinate different stages of life throughout the seasons. Investigating its full phenological cycle, not limited to a single stage, can help to reveal how and when maple acquires, allocates, or uses the energy over the growing season.

Like several deciduous species in extra-tropical climates, maple follows a sequential annual phenological cycle that alternates between dormancy and active growth phase. Dormancy ensures protection from cold and harsh environmental conditions but must be released before spring growth can resume (Basler et Körner 2014). In spring, freeze-thaw cycles promote pressure-driven sap flow within the xylem of maple trees (Graf et al. 2015). Maple syrup producers benefit from this process by collecting the sap to produce maple syrup using traditional gravity or modern vacuum tubing systems, with the latter widely adopted in large-scale operations for enhancing sap yield (Rapp et al. 2019). This season precedes the visible development of the meristems and serves as a physiological bridge between dormancy and growth. Budbreak usually coincides with the end of the sugar season (N'guyen et al. 2018) and signals the reactivation of photosynthesis and onset of primary growth. At this stage, with increasing transpiration from mature leaves and metabolic demand from different carbon sinks, water transport resumes (Christensen-Dalsgaard et Tyree 2014).

Sugar maple is a diffuse-porous deciduous hardwood species, characterized by evenly sized vessel pores throughout the growth ring. Within diffuse-porous

species, studies have reported contrasting patterns in the sequence of phenological events. In a study including maple, D'Orangeville et al. (2021) observed that canopy development may end before substantial radial growth begins. However, other studies on other diffuse-porous species (e.g., *Populus deltoides* and *Fagus sylvatica*) have observed a synchrony or only a short gap between the onset of leafing and the resumption of cambial activity (Deslauriers et al. 2009; Michelot et al. 2012). In contrast, in ring-porous species such as *Quercus pubescens*, xylem growth started before leaf expansion (Lavrič et al. 2017), with a large portion of annual growth completed even before full leaf expansion (Zweifel et al. 2006). These findings highlight that phenological sequences vary not only between the functional groups but also among species within a group. This underlines the need for further study in the specific phenological dynamics of sugar maple.

The period of sap exudation and budbreak in sugar maple have received substantial attention in the last decades (Buttò et al. 2023; Gao et al. 2025; Guo et al. 2020; Kurokawa et al. 2025), but the timings, coordination, and sequence of the other phenological events remain less understood. The timings of the sugar season were studied to relate sap yield with monthly temperatures, and to predict future development in a context of climate change (de Lima Santos et al. 2025). Furthermore, spring phenology was compared among different provenances (Guo et al. 2020), either to assess environmental drivers (Buttò et al. 2023), or climate-induced shifts in canopy development (Richardson et al. 2006). Recently, Bouchard et al. (2025) investigated early spring rehydration and water movement in leafless maples using stable isotopes, highlighting the role of root water uptake in xylem refilling and during the period of sap exudation. While these studies provide valuable

knowledge into specific phases, this fragmented approach limits understanding of the full annual rhythm of tree function. Since phenological events are interdependent, understanding their annual sequence is essential to assess how the shifts in their timing could affect carbon allocation for growth and reserve accumulation, and ultimately the potential of maple for sap production. In this study, we characterized the timings of phenological events in sugar maple to provide an integrated description of their annual sequence. We tested the hypotheses that (1) the sugar season ends at the reactivation of water transport in the xylem, (2) leafing occurs after the beginning of water transport, and (3) radial growth starts after the complete leaf expansion.

1.3 Materials and Methods

1.3.1 Study site

The permanent plot is located in a sugar maple stand in Simoncouche, QC, Canada (48˚13N, 71˚15W, 350 m a.s.l.), in the balsam fir-white birch ecological domain. It represents mixed forests growing on podzol soil. The climate of the area is typically boreal, with long, cold winters and short, warm summers (Rossi et al. 2011). Climate data from the local weather station over the past three decades indicate an average annual temperature of 2.9 °C, with mean minimum and maximum temperatures of -21 °C in January and 24 °C in July. Total precipitation was 945 mm, occurring in the form of rain. The snow cover mainly accumulates from November to April, reaching a maximum of up to 139 cm in January.

1.3.2 Tree selection and data collection

We randomly selected four dominant sugar maples to monitor stem diameter variation and sap exudation during 2018-2022 (Table 1). The selected trees had similar ages, stems free from visible damage, and a diameter at breast height (DBH) greater than 20 cm. The trees were never tapped before the beginning of the experiment. Each tree was equipped with an automatic point dendrometer (Agricultural Electronics Corp., Tucson, AR) installed on the stem at breast height (i.e., 1.3 m above ground). To minimize errors caused by hygroscopic thickness variations, bark was partially removed prior to installation. The dendrometers were set at a temporal resolution of 15 min, and the data were stored in a Campbell CR1000 datalogger (Campbell Scientific Corporation, Logan, UT). The dendrometer installed in tree 2 did not record data after June 2022, so we excluded the tree from

the analysis for 2022. The results for 2022 are based on data from the remaining trees with complete measurements.

The studied trees were equipped with a tipping bucket rain gauge (5222-L, TE525MM-L, Campbell Scientific Corporation, Logan, UT) to monitor the timings and volume of sap exudation throughout the sap season (Kurokawa et al. 2025). According to standard tapping procedures in Quebec, a notch (5 cm deep) was made on the stem 2 m above the ground using a drill. A plastic spout was then inserted and connected via plastic tubing to the rain gauge. Inside the rain gauge, the sap was directed into a small bucket (4.73 mL), which tipped over when filled with sap. After the measure, the sap flushed out of the rain gauge. To prevent rain, snow, or canopy debris from entering the rain gauge, each was covered with a tightly sealed cap. The rain gauges were equipped with data loggers that recorded sap volume at hourly intervals during the sugar season. We started with two rain gauges in 2018 and continued with four rain gauges in the following years. In 2022, we had technical problems with two rain gauges, thus these data were excluded from the analysis.

A standard meteorological station was installed to measure air temperature, soil temperature of the organic and mineral layer, snow depth and soil water content. The data were recorded every 15 minutes and stored as hourly averages in a data logger CR1000 (Campbell Scientific Corporation, Logan, UT).

Table 1 Characteristics of the sampled trees. Diameter at breast height = DBH.

Tree	DBH (cm)	Height (m)
1	34.5	16.9
2	20.5	9.4
3	25.5	14.8
4	33	16.7

1.3.3 NDVI extraction and calibration

We extracted polygons from the 1:20,000 Quebec Forest map (https://mffp.gouv.qc.ca/les-forets/inventaire-ecoforestier) and identified the polygons dominated by >70% of maple located in proximity to the study area. A time series of 250-m NDVI data from the Terra Moderate Resolution Imaging Spectroradiometer (MODIS) Vegetation Indices were acquired for 2018-2022 in the interval of 16 days. A double logistic function was fitted to the NDVI curve data for each year where time (t) was represented by day of the year (DOY):

$$\boldsymbol{NDVI = min + (max - min)\left(\frac{1}{1 + exp\left(-mS \times (t - S)\right)} + \frac{1}{1 + exp\left(mA \times (t - A)\right)} - 1\right)}$$

where *minNDVI* and *maxNDVI* are the minimum and maximum values of the NDVI, respectively; *S* and *A* are the two inflection points where the curve rises and falls; *mS* and *mA* are the growth rates associated to the inflections point (Khare et al. 2019).

The curves were standardized to a range of 0–1 and used to identify the phenological events of budbreak and full leaf expansion using the thresholds proposed by Buttò et al. (2023). i.e., when NDVI reached 0.63 and 0.77, respectively. Buttò et al. (2023) validated these thresholds using both field observations and NDVI data for the same study species, making this method reliable for our study despite the lack of on-site field observations. Similarly, leaf fall was defined when NDVI reached 0.50 (White et al. 2009).

1.3.4 Statistical analysis

The data extracted by the rain gauges and dendrometers were converted into percentages and fit by piecewise regressions using the segmented package in R to identify the two major breakpoints representing the onset and ending of sap production season and radial growth.

For each day, dendrometer values of the stem diameter variation were normalized by setting the daily minimum diameter to 0 and the daily maximum to 100. We examined the hourly variations in stem diameter to identify the normal and inverted daily cycles according to Turcotte et al. (2009). The normal cycles had nighttime stem expansion and daytime contraction, reflecting the typical plant water dynamics with nighttime reductions in transpiration that allow for water replenishment of the stem. The inverted cycles were marked by a daytime expansion and a nighttime contraction of the stem following the daily variations in temperature (Turcotte et al. 2009). The shift of daily stem diameter pattern from inverted to normal cycles was used as the proxy for the transition from positive pressure (sap exudation) to negative tension (xylem water transport). We defined the season with normal cycles as the one characterizing water transport by the xylem.

The temporal distribution of each phenological event was estimated using normal distributions, based on the mean and standard deviation of the day of year (DOY). These distributions highlighted the timing and variability of each phenological phase across multiple years. The Shapiro-Wilk W test was used to evaluate the assumption of normality for each phenological event. To statistically assess the null hypothesis, p-values > 0.05 were considered a significant deviation from normality.

Quantile-quantile (Q-Q) plots were visually analyzed to detect any deviations from normality.

We conducted an ANOVA and a post-hoc Tukey's HSD test on phenological events to examine differences among years, with the tree included as a random effect. Phenological events were compared using paired t-tests and Principal Component Analysis (PCA). In the PCA, raw values of the phenological variables (DOY of each event) were used without centering or scaling. All statistics were performed in R and JMP Pro 14 (SAS Institute Inc., Cary, NC).

1.4 Results

1.4.1 Timing of sugar season

The sugar season started between late March and mid-April (DOY 81-107) and ended in May (DOY 106 -139). On average, the sugar season started on DOY 94 ±10 and ended on DOY 123 ± 11, indicating comparable interannual variability between the two phenological events (Fig. 1.1).

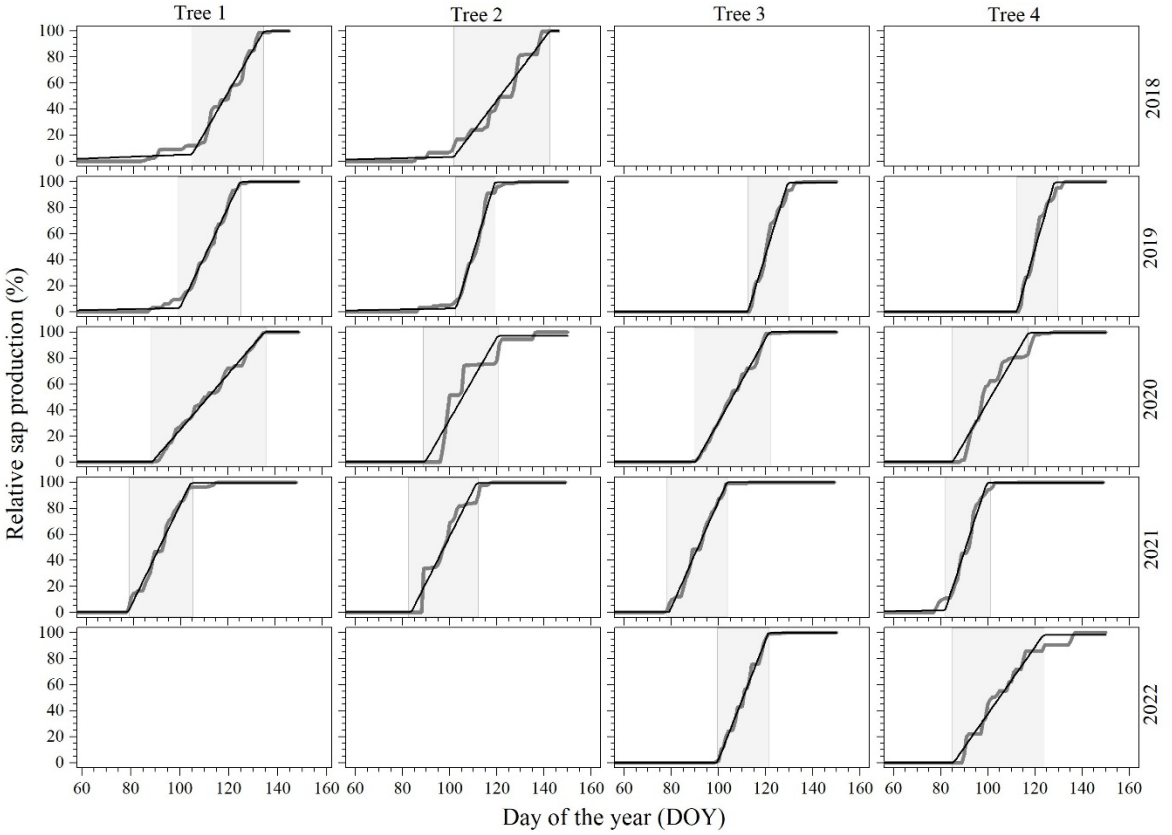

Fig 1.1. Timing of onset and ending of sugar season across the study years and trees. Grey curve represents the cumulative sap water production and black curve represents the fitted segmented model; the first and second vertical lines represent the day

ANOVA showed significant interannual differences among years in both onset ($F = 15.26$, $p < 0.05$) and ending ($F = 11.38$, $p < 0.05$) of the sugar season (Table S1). Post hoc comparisons showed an earlier onset of the sugar season in 2021 (DOY 81) than 2018 (DOY 103) and 2019 (DOY 107) (Fig. 1.2).

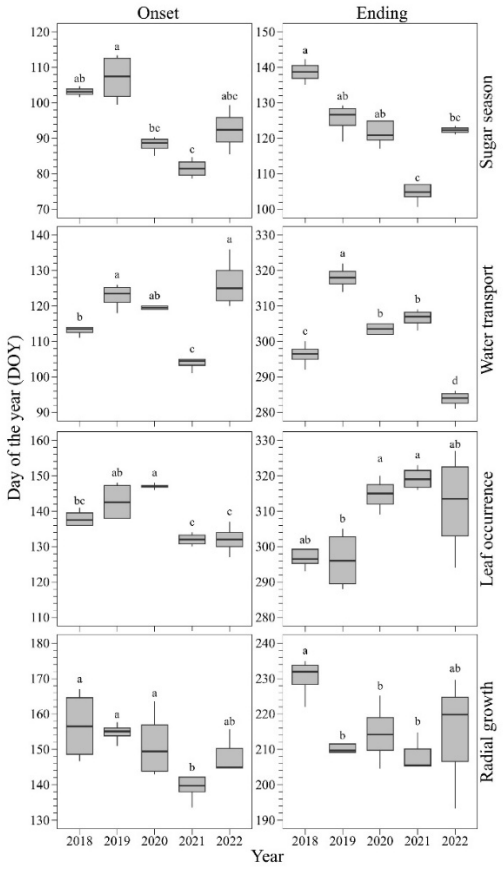

Fig 1.2 Timing of onset and ending of phenological events for the different study years 2018-2022. Box plot represents the upper and lower quartiles, with whiskers indicating the 10th and 90th percentiles and the result of post hoc test is indicated by the letters above the boxplot. The medians are indicated by a black horizontal line.

The earlier sugar season onset corresponded with an earlier snowmelt and the consequent earlier increase in soil water content (Fig. 1.3). The earliest sugar season ending occurred in 2021 (DOY 106), when snow had disappeared and soil temperatures started warming up. On average, the sugar season lasted from 18 days in 2019 to 36 days in 2018. Despite the short sugar season, 2019 exhibited the highest sap yield (24.88 L) (Fig. S1). Other good sap yields were observed in 2021 (13.45 L) and 2020 (12.37 L). Conversely, 2022 recorded the lowest sap yield (4.95 L). The year 2018, with the longest sugar season, produced a moderate volume of sap (7.82 L) (Fig. S1). The thicker and thinner snow covers were recorded in 2022 and 2021, reaching 1.17 and 0.47 m, respectively. Snow started melting a few days before the sugar season onset and disappeared completely at the end of sap exudation. During that period, soil water content increased up to 0.58 cm^3/cm^3 in 2018 (Fig. 1.3). On average, minimum and maximum temperatures during the sugar season were -3.90 and 7.34 °C, respectively (Fig. 1.3).

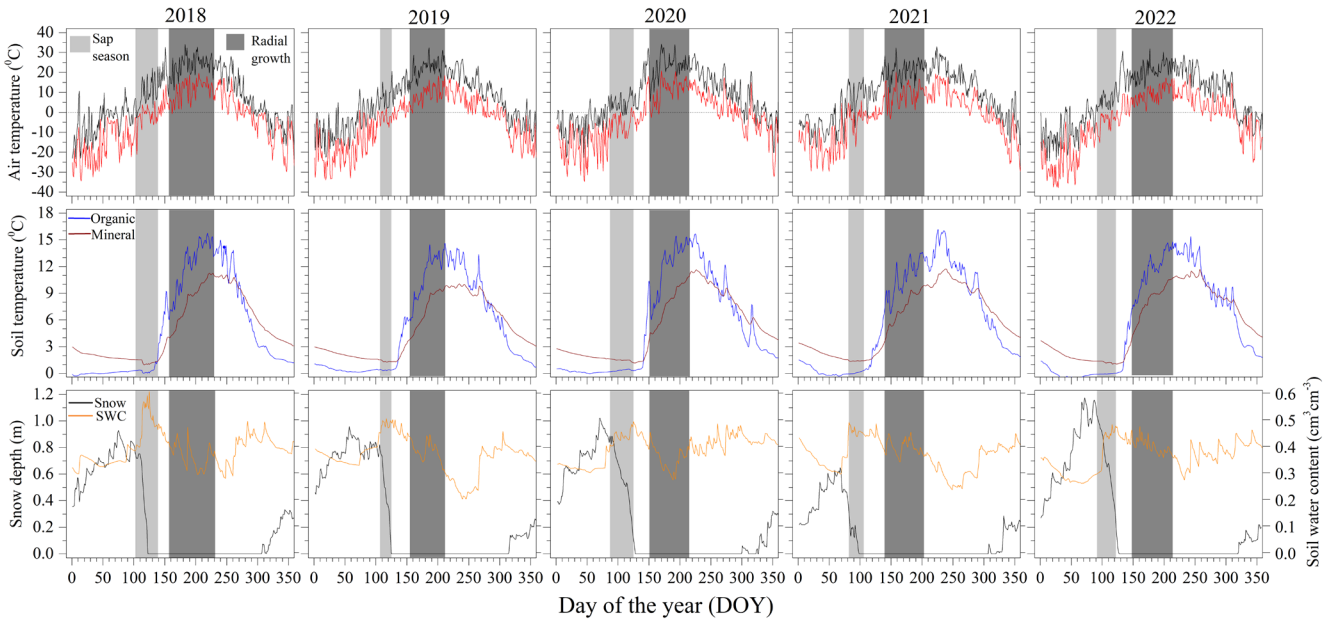

Fig 1.3 Maximum (black line) and minimum (red line) air temperatures, soil temperatures in organic (blue line) and mineral (brown line) layer, snow depth (black line), and soil water content (orange line). The two shaded areas represent the estimated period of sugar season and radial growth respectively from 2018 to 2022.

1.4.2 Radial growth

Radial growth started between late May and early June (DOY 140-157) and ended in August (DOY 203-230) (Fig. 1.4). On average, radial growth began on DOY 150 ± 6 and ended on DOY 215 ± 9, which indicated a slightly higher variability in the ending than onset of growth (Fig. 1.4). The effect of the year on the timing of radial growth was significant, with F values of 10.13 for the onset and 8.61 for the ending ($p < 0.01$; Table S1). Post hoc tests showed significant variation in the timing of the growth period (Fig. 1.2). Radial growth started earlier in 2021 (DOY 140) and 2022. The latest ending of growth was observed in 2018 (DOY 230) and 2022.

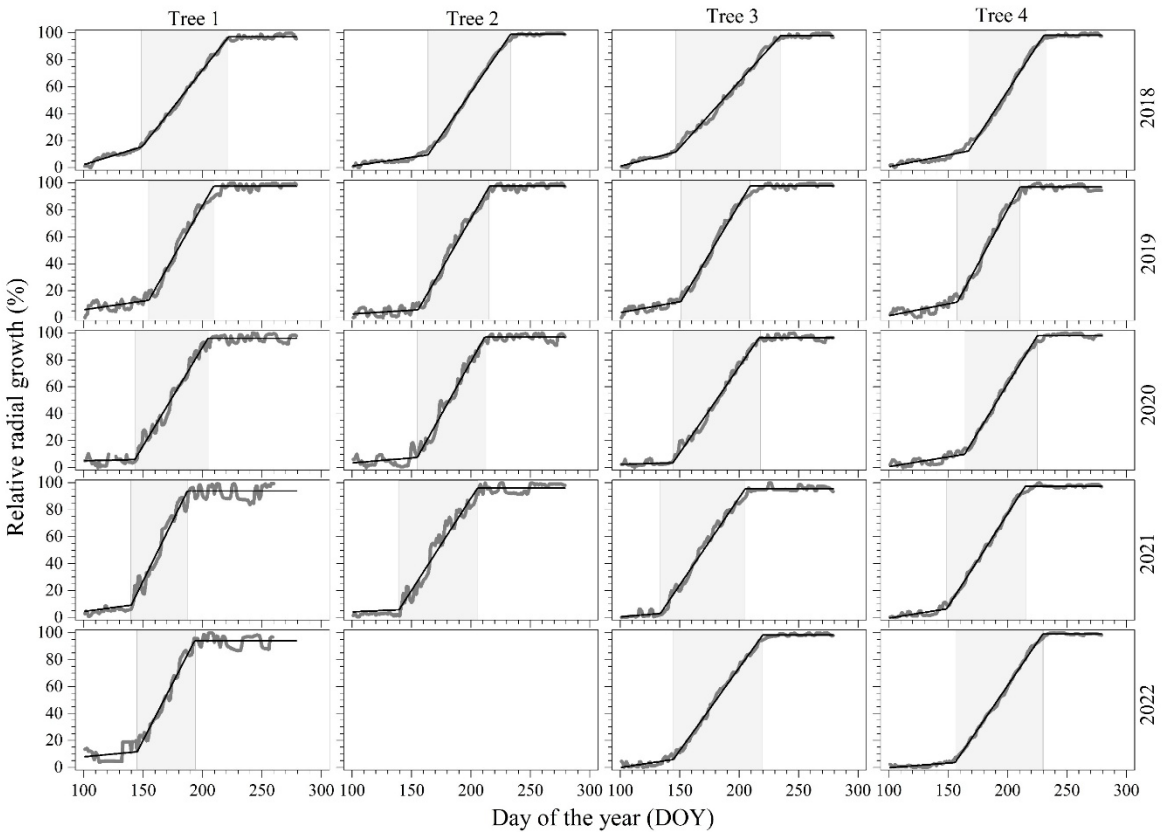

Fig 1.4 Timing of radial growth for the study years (2018-2022) and trees. Grey curve represents dendrometer measurements and black line represents the fitted segmented model; the first and second vertical lines represent the day of onset and ending of radial growth respectively and the radial growth period shown by shaded grey area.

On average, we calculated 64 days of radial growth, ranging from 56 days in 2019, to 73 days in 2018. Growth varied across the years, with the highest amplitude observed in 2018 (3.53 mm, SD = ± 0.57mm), corresponding to the longest growing season. Conversely, the minimum growth was observed in 2021 (1.41 mm), the year with the shortest season (Fig. S1). The year 2019 experienced the coldest spring, especially in March, with the average temperature dropping to -

7.67 °C. Before the onset of radial growth, we observed a complete disappearance of snow and an increase in soil temperature. During the period of radial growth, the organic and mineral layers showed temperatures of 6-16 °C and 3-12 °C, respectively (Fig. 1.3).

1.4.3 Leaf phenology

The annual pattern in NDVI followed a characteristic bell-shaped curve, with a gradual increase in spring, a plateau in summer and a decline in autumn, showing the phenological events of seasonal leaf development (Fig. S2). The double-logistic model provided a good fit, with high correlations (R^2 = 0.98-0.99, $p < 0.001$) between observed and predicted NDVI values. Based on the methods of previous studies, the timings of budbreak and leaf occurrence were identified at the relative height of 0.63 and 0.77, respectively, whereas the date of leaf fall was estimated at 0.5.

Budbreak was observed from DOY 117 in 2021 to DOY 134 in 2020, with an average onset occurring on DOY 126. Leaf expansion occurred 12 days after budbreak, between DOY 132 and 147 (average on DOY 138). The shortest and longest interval between budbreak and leafing was observed in 2022 (9 days), and 2021 (15 days), respectively. A significant difference between the years was observed from a post hoc comparison for both leaf expansion ($F = 14.94$, $p < 0.01$) and leaf fall ($F = 4.97$, $p < 0.05$) (Fig. 1.2 and Table S1). Leafing occurred earlier in 2021 and 2022 (DOY 132) than in 2019 (DOY 143) and 2020 (DOY 147). The earliest leaf fall was observed in 2019 (DOY 296) while the latest leaf fall occurred in 2021 (DOY 320). On average, the complete canopy lasted 170 days, ranging from 153 days in 2019 to 187 days in 2021.

To assess whether phenological timing varied across spatial locations, a separate one-way ANOVA was conducted for the study polygons (Table S2). This analysis revealed no significant differences in the timing of budbreak, leaf expansion and leaf fall among polygons (all $p > 0.05$; Table S2), which confirmed that leaf phenology was consistent across the region.

1.4.4 Water transport in trees

The studied trees showed very similar seasonal and daily patterns in stem diameter. The variation in stem diameter followed a typical seasonal pattern, with a slow increase in spring until the end of May, and a quick growth until July. The plateau in the curve observed in August marked the end of the radial growth in maple. The diurnal fluctuations provided an indirect way to identify the onset of water transport in spring, characterized by daytime shrinkage and nighttime swelling. This pattern persisted until autumn, when the nighttime shrinkage and daytime swelling indicated the cessation of water transport in trees. The onset of water transport occurred between mid-April and early May (DOY 104 –126) and lasted until mid-October to mid-November (DOY 284 – 318). On average, water transport was estimated to occur from DOY 117 ± 8 to 301 ± 12 (Fig. 1.2).

ANOVA showed significant differences among years in both the onset ($F = 24.94$, $p < 0.01$) and ending ($F = 76.12$, $p < 0.01$) of water transport. Post hoc comparisons showed an earlier onset in 2021 (DOY 104), and later onsets in 2019 and 2022, on DOY 123 and 126, respectively. The year 2022 exhibited an earlier ending of water transport (DOY 284). The later cessation of water transport was observed in 2019 (DOY 318) (Fig. 1.2).

1.4.5 Temporal sequence of phenological events

The Shapiro-Wilk test produced values ranging between 0.92 and 0.98 for all phenological events. The p-values of the available dataset were not significant ($p > 0.05$), indicating no deviation from normality. The temporal sequence of phenological events had a distinct seasonal pattern (Fig. 1.5). The sugar season marked the first phenological event, initiating in early spring. The end of the sugar season corresponded to the onset of water transport and budbreak ($t = 1.48$ and $t = 1.82$, respectively; $p > 0.05$). The emerging leaves were completely expanded three weeks after the onset of water transport in the stem. Radial growth began 12 days after full leaf expansion and 29 days after the end of the sugar season (DOY 123 ± 11 versus 150 ± 6). The paired t-test confirmed a significant difference between these two phenological phases ($t = 10.9$, $p < 0.001$). Radial growth stopped at the beginning of August (on DOY 214), while the leaves persisted for nearly three months, extending the period of canopy cover until October. Leaf fall and the cessation of water transport in the stem occurred within the same period, as also demonstrated by the lack of differences between the timings of these two phenological events ($t = 1.70$, $p > 0.05$).

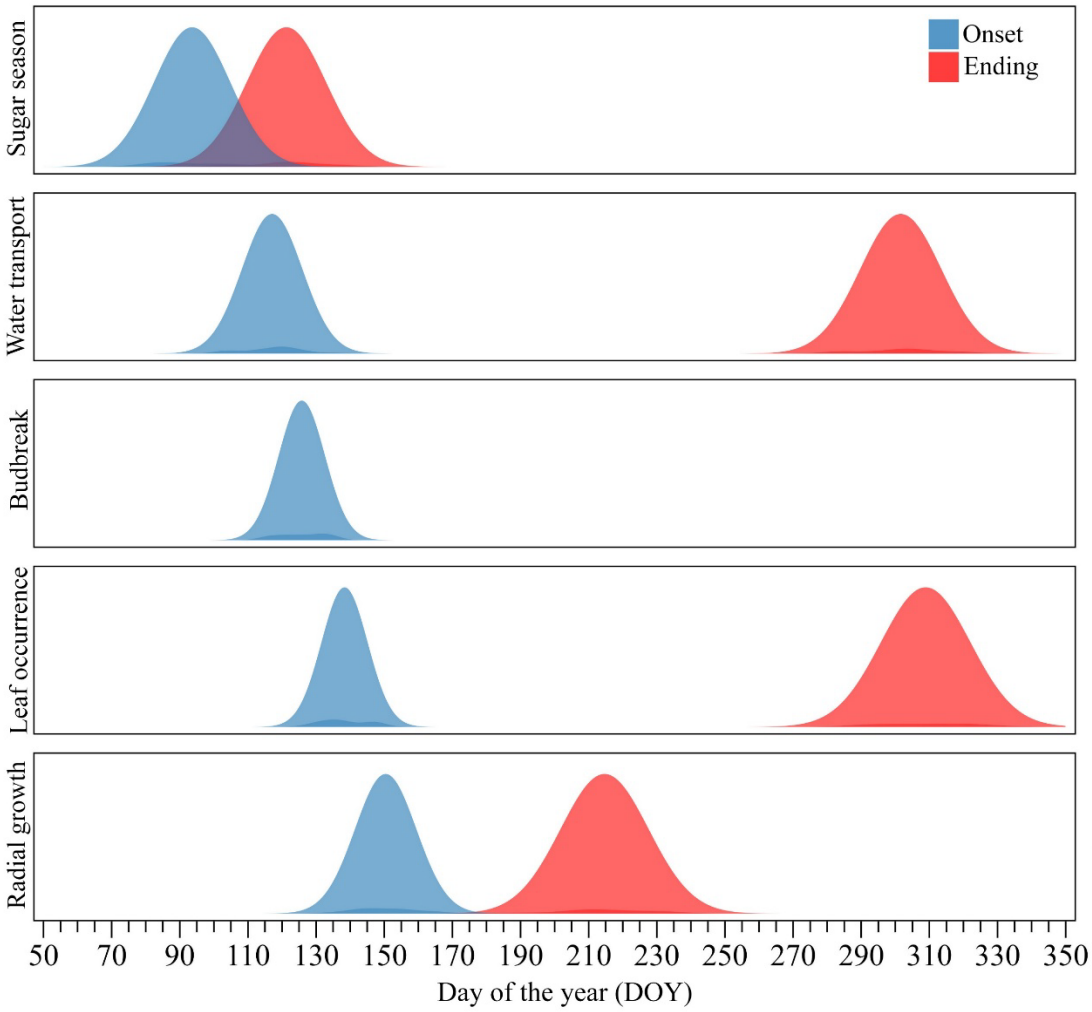

Fig 1.5 Schematic diagram of the timing of the phenological events studied. The normal distribution plots show event timing based on rain gauge, dendrometer and remote sensing data.

The principal component analysis (PCA) summarizes the relationship between the events. The PCA calculated on the phenological events produced two axes (PC1 and PC2) explaining 70.42% of the total variance (Fig. 1.6). PC1 and PC2 explained 50.97 and 19.45% of the variance. The phenological events in spring, including the sugar season, budbreak, water transport and leafing, were mainly represented by PC1. The spring events had similar direction, suggesting good correlations and

temporal synchrony among them. More specifically, the onset of radial growth and ending of the sugar season were closely aligned, indicating a strong correlation between the two events. Leaf fall showed a positive correlation with PC1, suggesting a negative relationship with the spring events. The phenological events in autumn, such as leaf fall or the ending of radial growth were mainly correlated with PC2, suggesting no relationships with the spring events. The cumulative sap volume had a negative correlation with the growth amplitude, as indicated by their diverging directions calculated by the PCA (Fig. 1.6).

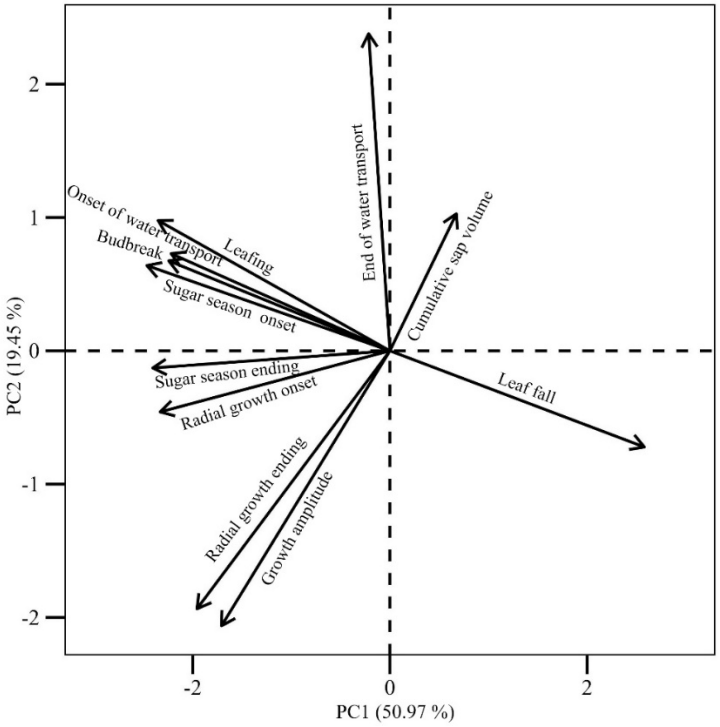

Fig 1.6 Principal components analysis (PCA) biplot of the relationship of phenological events. The axes represent the first two principal components (PC1: 50.97%, PC2: 19.45%). Arrows indicate the direction and strength of the contribution of each variable to the principal components.

1.5 Discussion

This study investigated the timings of spring and autumn phenology in sugar maple. We collected data for five years (2018 - 2022) to describe and understand the sequence, chronological order and synchrony of phenological events. We confirmed the hypothesis that the sugar season ends with the onset of water transport, followed in turn by leafing. Unlike our hypothesis, radial growth and leafing was mismatched, by a lag of approximately two weeks.

1.5.1 The sugar season and the water transport

The sugar season started at the end of March, when maximum daily temperatures exceeded freezing point and snow started melting, resulting in a consequent increase in soil water content. In that period, the soil, still completely or partially covered with snow, had a constant temperature close to freezing point. Sap exudation occurs during the freeze-thaw cycles, which generate positive pressures in the xylem (Graf et al. 2015). Such pressure facilitates water uptake by the roots and rehydrates the aboveground tissues following winter dormancy (Niu et al. 2017). The water derived from the snowmelt contributes significantly to the sap during the sugar season (Bouchard et al. 2025). Accordingly, Robitaille et al. (1995) observed a decline in sap exudation during periods of deep soil freezing, highlighting the importance of adequate root water access for sap exudation. Our results confirm the role of the concurring events of freeze-thaw cycles, snowmelt and increasing soil water content for sap exudation (Bouchard et al. 2025; Kurokawa et al. 2025) and spring rehydration (Nehemy et al. 2022), although such observations were still unable to disentangle the main driver of the sugar season.

Tension-driven water transport in trees resumed in the second half of April, corresponding with the end of the sugar season. The synchronism of these two phases marks a physiological transition in xylem function from pressure-driven sap exudation to tension-driven, active hydraulic transport (Melcher et al. 2003). During this transition, we observed the complete disappearance of snow and a rapid rise in soil water content. During winter, the freezing-induced embolism disrupts the water conductivity by forming gas or air bubbles in the xylem (Tyree et Cochard 1996). In spring, xylem needs to recover from the embolism to resume water transport and growth, which can occur through the refilling of the embolized vessels through various mechanisms (Cochard et al. 2001). In species with diffuse-porous wood, such as maple, the reparation of embolism occurs through positive xylem pressure generated in the roots (Graf et al. 2015; Niu et al. 2017). Sperry et al. (1988) observed that the embolism in maple seedlings decreased to approximately 20% by June and was associated with positive pressure originating from roots. Significant embolism recovery from a similar mechanism has also been reported in other diffuse porous species such as *Betula pendula*, *Betula papyrifera and Alnus crispa* (Hölttä et al. 2018; Sperry et al. 1994). Niu et al. (2017) observed that several diffuse porous species capable of generating positive root pressure exhibited nearly complete recovery from winter embolism. These findings in maples and other diffuse-porous species belonging to the genus *Betula* and *Alnus* may suggest a common recovery mechanism from embolism prior to the onset of xylem water transport among cold-adapted deciduous trees.

The positive pressure generated by the roots in maple contributes to the recovery from winter embolism (Sperry et al. 1988). This recovery results in the onset

of tension-driven water transport marking the end of pressure-driven sap flow from the trees (Melcher et al. 2003). Following this transition, sap can no longer be extracted from the tree, thus concluding the sugar season, which is defined by the beginning of xylem recovery and the onset of tension-driven water transport.

1.5.2 Water transport and leaf phenology

The tension-driven water transport started at the beginning of May, followed by budbreak and leafing in mid-May. Budbreak occurred earlier in 2021, which is in agreement with previous observations carried out in the same region (Gao et al. 2025). The earlier onset of budbreak did not result in an earlier leaf expansion. The year 2021 exhibited the longest interval between budbreak and leafing, exceeding that of all the years. This observation suggests diverging influences of the environment on the different phases of leaf phenology, which could be attributed to the conservative strategy of maple to avoid potential damage of late spring frost on the developing tissues (Buttò et al. 2023).

We recorded a lag of two weeks between the onset of tension-driven water transport and leafing. Our observations align with previous findings in *Acer pseudoplatanus*, where water in the stem increased progressively before budbreak (Essiamah et Eschrich 1986). In *Betula platyphylla* and *Salix sachalinensis*, approximately 10% of the xylem vessels remained cavitated by the time of full leaf expansion, indicating that maximum embolism recovery occurs before the onset of leaf transpiration (Utsumi et al. 1998). These observations suggest that tension-driven water transport likely requires the refilling of the xylem to support rehydration of the bud meristems in preparation for budbreak.

A study done in species with ring-porous and diffuse-porous wood showed contrasting results on the relationship between stem water transport and leaf phenology (Suzuki et al. 1996). In the former and latter species, the new vessels are produced before and after leafing, respectively, suggesting that the xylem of the previous year plays a leading role in early spring water transport (Suzuki et al. 1996). Regardless of the wood structure, tension-driven water transport can resume either concurrently with the formation of new vessels or the refilling of existing ones, but both strategies ultimately lead to the restoration of hydraulic efficiency to support leaf development (Niu et al. 2017). This water movement occurring in early spring supports rehydration of the buds, and contributes to the swelling of the apical meristems, ultimately resulting in budbreak and leafing (Essiamah et Eschrich 1986). The onset of tension-driven water transport has been linked to the recovery of embolized vessels after the winter, which is required for an efficient hydraulic conductivity and transpiration (Utsumi et al. 1998). Similar observations in *Malus domestica* showed that delayed xylem refilling under soil frost conditions postponed both leafing and cambial activity, highlighting that hydraulic recovery is a physiological prerequisite for spring phenology (Beikircher et al., 2016). The formation of functional vessels is essential to restore hydraulic continuity and sustain the water movement needed for the expansion of developing leaves (Lavrič et al., 2017). These observations suggest that tension-driven water transport likely requires the refilling of the xylem to support rehydration of the bud meristems in preparation for budbreak.

1.5.3 Leafing and radial growth

At the end of May, approximately two weeks after leafing, we recorded the beginning of radial growth in the stem. At that time, the snow had completely melted, and soil temperature started increasing. The observed lag between leafing and the onset of radial growth is in agreement with several previous studies on diffuse-porous species, although the lag between leafing and radial growth seems to be inconsistent across species. In *Acer platanoides*, *Populus deltoides* and *Fagus sylvatica*, radial growth typically initiates with, or shortly after, canopy development (Deslauriers et al. 2009; D'Orangeville et al. 2022; Michelot et al. 2012; Prislan et al. 2013), while wider lags (4-7 weeks) were reported in *Corylus avellana* (Pasqualotto et al. 2022), and *Carpinus betulus* (Klein et al. 2016). Overall, these studies suggest that, despite a similar sequence of phenological events, substantial differences among species can exist.

The relationship between leaf phenology and cambial activity remains an attractive topic in forest ecology. Studies conducted across functional groups have yielded contrasting results (Silvestro et al. 2025). In evergreen conifers, cambial activity precedes needle unfolding (Antonucci et al. 2015; Michelot et al. 2012; Rossi et al. 2009). Also, ring-porous species often resume growth before budburst, a strategy linked to the need to restore a functional xylem after the embolisms occurred in winter (Sperry et al. 1994). Vessels of ring-porous species are dismissed after one season (Kudo et al. 2018), requiring an early cambial division to ensure that the hydraulic system is restored before reactivation of the transpiration in spring. In contrast, diffuse-porous species like maple retain functional xylem vessels for multiple years due to their greater resistance to embolism. Maple can then delay cambial reactivation (Suzuki et al. 1996), thus relying more on current year

photosynthates to support radial growth. For instance, *Fagus sylvatica* reaches its maximum radial growth in June (Michelot et al. 2012), when both leaf mass per area and photosynthetic capacity reach their maximum (Eglin et al. 2009). This pattern is consistent with observations in conifers, where the highest rate of radial growth corresponds to the peaks of cell division and tracheid in cell enlargement, a process primarily driven by turgor pressure and dependent on water availability (Cuny et al. 2015). This initial phase of growth in volume, occurring in late spring and early summer, is followed by the phases of secondary wall thickening and lignification, which require higher supply of sucrose to support cell-wall formation (Silvestro et al. 2025). The phase of growth in biomass, occurring in summer and early autumn, represents the most carbon-demanding step of wood formation. Importantly, secondary wall formation and thickening occur with a marked delay compared to the expansion in stem diameter initiated by cell division and enlargement (Cuny et al. 2015), and are predominantly supported by newly assimilated carbohydrates, as evidenced by their close synchrony with peak photosynthetic activity (Silvestro et al. 2024). Our measurements, conducted with dendrometers on the stem, recorded the growth in volume, but were unable to detect the last process of wood formation, i.e. the growth in biomass, which requires other sampling techniques (Silvestro et al. 2025). The two-week lag between leaf emergence and onset of radial growth marks a developmental transition from primary growth and secondary growth with different prioritization of carbon allocation in maple.

1.5.4 Ending of radial growth and leaf fall

Radial growth, i.e. growth in volume of the stem, ceased in early August, while leaves remained active for more than two additional months. This mismatch is consistent with other species (Čufar et al. 2008; Prislan et al. 2013). While cambial activity halts in response to shorter photoperiod, photosynthesis continues as long as leaves remain functional. The gap between the ending of radial growth and leaf fall reflects a shift in resource allocation towards other processes, including secondary cell wall formation and lignification and accumulation of reserves, which are major carbon sinks in trees (Cuny et al. 2015). The cessation of radial growth prior to leaf senescence likely reflects internal physiological thresholds, combined with a need (i) to prioritize storage for the frost hardiness in preparation for the winter stress, and (ii) to ensure sufficient time for the lignification of latewood following the end of cell division in early summer. The reserves play a crucial role in enhancing cold hardiness and ensuring survival through winter, as well as supporting subsequent early spring processes such as budburst, flowering and cambial reactivation (Mura et al. 2025). These same carbohydrate reserves, remobilized during early spring to support metabolic reactivation and growth resumption, will then contribute to the sugar content of xylem sap collected for maple syrup production.

Both leaf fall and the cessation of tension-driven water transport occurred at the beginning of November. This period is preceded by leaf senescence, which involves the degradation of chlorophyll. During this process, the nutrients, especially nitrogen and magnesium, are remobilized from the leaves and redistributed to storage tissues, primarily roots and shoots (Dox et al. 2021). Chlorophyll degradation

results in loss of green pigments, revealing other non-green pigments, such as carotenoids (Croft et al. 2014). As leaf senescence progresses, phloem transport is blocked by the formation of an abscission layer and deposition of callose at the base of the petiole (Fracheboud et al. 2009), while the expanding parenchyma cells occlude the vessels, progressively sealing off the water supply (Brodersen et al. 2010). Our study provides evidence of the relationship between the cessation of tension-driven water transport and leaf fall in maple. In *Castanea sativa,* a decline of 88% was recorded in stem hydraulic conductance before visible leaf senescence and was linked to vessel blockage caused by tylose formation (Salleo et al. 2002). As senescence progressed and leaves started changing their color, a significant reduction in petiole hydraulic conductance was also observed, associated with the progressive blockage of xylem vessels in the petiole. This finding suggests that the hydraulic shutdown may not only be the consequence of a senescence process but may also have a facilitating role in leaf detachment (Salleo *et al.* 2002). The loss of water transport likely contributes to protecting stem tissues from freeze-induced damage during winter (Tyree et Cochard 1996). Similar results in maple may suggest a coordinated shutdown of vascular function, representing a physiological transition into dormancy to ensure survival during the harsh conditions of winter.

1.6 Conclusion

This study provides an integrated description of sugar maple phenology based on five years of observations. We showed that the sugar season ends with the onset of tension-driven water transport, marking a physiological shift from pressure-driven sap exudation to tension driven water transport, thus creating the necessary conditions for reactivation of the primary (apical) and secondary (lateral) meristems. The synchronism of these two events suggests that sap production beyond this transition is unlikely to increase the total sap yield irrespective of the tapping techniques or technologies used. These results highlight the importance of assessing the weather signals driving sap production in maple and aligning the tapping period with the optimal time window to maximize sap yield.

The onset of tension-driven water transport was followed by leafing and radial enlargement of the stem, which indicated the need to recover hydraulic conductivity before growth reactivation. While stem growth ended by early August, leaves remained photosynthetically active until October-November, supporting carbon accumulation in the form of biomass in wood and reserves, and preparing the organs for winter conditions. This natural synchronization is crucial for the process of sap production in spring, which relies on the sugars accumulated during the previous summer and autumn, and profits from a short time window when root pressure builds up before the beginning of leaf development and transpiration. Producers should be ready to synchronize the tapping dates with the reactivation of maples to profit from the period most favorable for sap exudation.

In the context of climate change, earlier warming, alteration of freeze–thaw cycles, and reduced snowpack will affect dates and duration of the sugar season, with

potential consequences for carbohydrate reserves and sap yield. Despite the good adaptation of sugar maple to the local climate, its dependence on snowmelt and sensitivity to spring frost highlights potential vulnerabilities. Adaptive management strategies, including the assessment of the best tapping period according to the environmental signals, might be crucial to sustain productivity. The sequence and linkages of the phenological events observed in this study can effectively guide adaptive strategies for the maple industry. A detailed monitoring of the environmental signals, e.g. snow melting or the occurrence of freeze-thaw cycles, and the phenological events in maple, e.g. complete stem rehydration or the first phases of bud swelling that may indicate the end of the sap season, can help producers to optimize the operation dates rather than relying solely on the historical calendars. Overall, a deeper understanding of maple phenology will be crucial for adapting tapping practices, sustaining maple syrup yields, and, in general, the economic viability of the sugarbush operations facing the increasingly inter-annual variability of weather conditions.

1.7 CRediT authorship contribution statement

Rachana Bhandari: Writing – review & editing, Writing – original draft, Visualization, Software, Formal analysis, Data curation, Conceptualization. Roberto Silvestro: Writing – review & editing, Writing – original draft, Conceptualization. Sergio Rossi: Writing- review and editing, Supervision, Project administration, Methodology, Resources, Funding acquisition, Conceptualization.

1.8 Declaration of Competing Interest

The authors declare that they have no known competing financial interests or personal relationships that could have appeared to influence the work reported in this paper.

1.9 Acknowledgements

The authors thank S. Kurokawa, E. Gharbia, F. Gionest, P. Nadeau, H. McNulty for technical support, and A. Garside for checking the English text.

1.10 Funding

This research was supported by the Natural Sciences and Engineering Research Council of Canada (research programs Alliance and Discovery grants), Fonds de Recherche du Quebec – Nature et Technologies (AccFor, project no. 309064), Fonds de recherche du Québec – Société et culture, Observatoire régional de recherche en forêt boréale, Créneau d'excellence en acériculture, Club acéricole du Sud du Québec, Syndicat des producteurs de bois du Saguenay–Lac-Saint-Jean, Producteurs et productrices acéricoles du Québec, Centre ACER, and Fondation de l'Université du Québec à Chicoutimi.

1.11 Data availability

The data supporting the findings of this study will be available in Borealis, the Canadian Dataverse, after the final acceptance for publication.

1.12 Supplementary materials

Table S1. Effects of Year (Y) on different phenological phases of sugar maple evaluated by ANOVA models. Tree is treated as a random effect in the model. Values are F-statistics from ANOVA.

Phenological event	Phase	Year
Sugar season	Onset	15.26**
	Ending	11.38**
Radial growth	Onset	10.13 **
	Ending	8.61 **
Water transport	Onset	24.94**
	Ending	76.12**
Leaf occurrence		14.94**
Leaf fall		4.97*

* $P < 0.05$; ** $P < 0.01$.

Table S2. Effect of sites (polygons) on different leaf phenological events in sugar maple evaluated by one way ANOVA models.

Leaf phenology	F-value	P value
Budbreak	0.1112	0.95
Leaf occurrence	0.204	0.89
Leaf fall	0.156	0.92

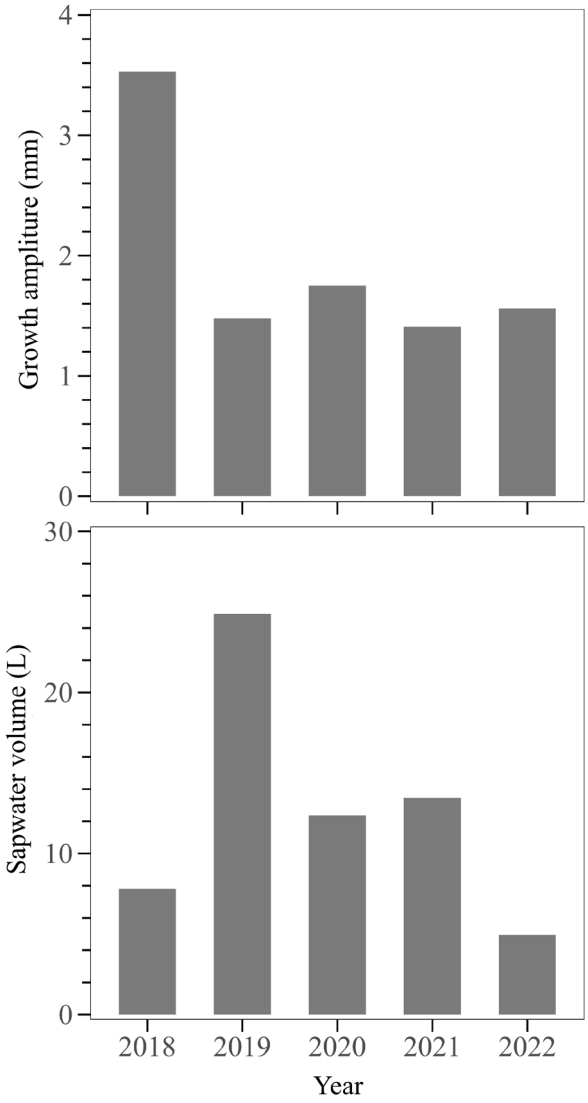

Fig S1. Total average volume of sap and average growth amplitude of the studied tree for five years (2018-2022).

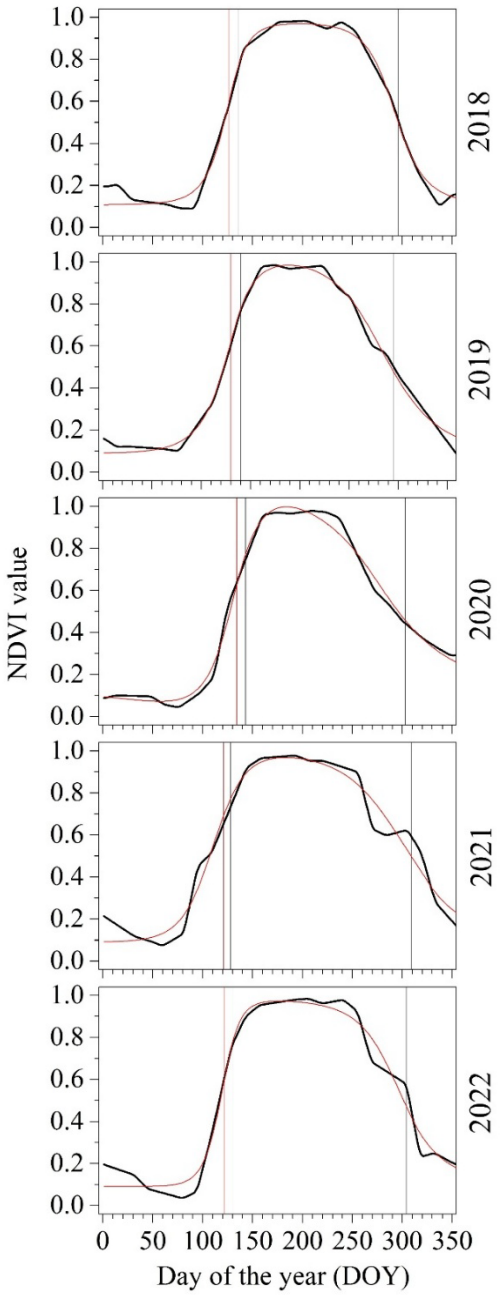

Fig. S2. The timing of budbreak, leaf occurrence and leaf fall derived from NDVI data where the black line represents the raw NDVI data over time and the red line represents the fitted logistic function. The red and black colored lines represent the DOY of budbreak, leaf occurrence and leaf fall respectively.

CHAPTER II

Testing phenocam for monitoring autumn phenology in sugar maple

2.1 Abstract

Digital repeat photography derived from PhenoCam offers a reliable source of near ground observations with frequent and high-resolution data for monitoring vegetation phenology. These tools serve as an excellent proxy for near ground observations and allow for detailed comparisons of phenological events. This study aims to study the reliability of phenocam to study the timing of autumn leaf phenology by comparing three phenocam derived indices (green chromatic coordinate (GCC), red chromatic coordinate (RCC) and excess green index (ExG)) in sugar maple (Acer Saccharum Marsh). We also recorded the stages of autumn phenology twice a week. The study was conducted in autumn of 2023 in Quebec, Canada. GCC and ExG were proved to be the best indicator in detecting the onset of leaf color change. Whereas RCC best predicted the timing of leaf fall in the study area. This study highlights the use of digital cameras instead of labor-intensive field based phenological monitoring. These findings are useful for planning phenological observations in remote areas, areas with extreme weather conditions where regular human observation is not possible.

2.2 Introduction

Leaf senescence is a key stage in plant development. It begins with a decline in leaf function, starting from color change and concluding to leaf fall (Keskitalo et al. 2005). The first stage during the leaf senescence is the degradation of chlorophyll which includes the recovery of the valuable nutrients from the leaves. The degradation of chlorophyll results in the domination of other non-green pigments such as carotenoids (Keskitalo et al. 2005). This final phase in leaf phenology involves the creation of an abscission or the separation layer in the petiole compressing the phloem and sealing of xylem through the expanding parenchyma tissues (Fracheboud et al. 2009). Most sugar maple phenology studies use remote sensing or short field monitoring data, so the link between near ground PhenoCam color data and detailed leaf stages is not well defined in this species.

The onset of leaf senescence can be studied by several processes such as assessment of leaf nutrient relocation, chlorophyll degradation or the measurement of leaf color change from the human observations (Keskilatio et al. 2005). Field-based data collection is considered more reliable and traditional way of obtaining accurate and fine resolution phenological events (Xie et al. 2018). However, this approach may be inappropriate for inaccessible and remote areas experiencing extreme weather conditions. Further, satellite-based data are widely used to detect the timing of phenological events (Jiang et al. 2022; Khare et al. 2019; Wang et al. 2020). While offering a broader and more reliable perspective, the quality of data generated may be limited by the presence of clouds and other airborne particles,

leading to lower-quality images (Li et al. 2023). In this scenario, near-ground digital cameras capturing frequent images of vegetation canopy multiple times a day have proved to be a reliable way to obtain accurate and consistent information of phenological changes in plants (Khare et al. 2022).

Digital repeat photography commonly done by PhenoCams has been an accessible tool because of its low cost, easy installation process in the field, high resolution and frequent observations (Zhang et al. 2020). These cameras provide high resolution images in red, green, and blue (RGB) channels and the analysis of these channels can provide the change in different leaf phenological events (Richardson et al. 2009). The PhenoCam comes out as a more reliable tool than the field observations to study leaf phenology due to its temporal and spatial resolution (Khare et al. 2022). These cameras can be more useful in the remote and inaccessible areas or the sites with harsh climates. Recently, many studies have used the combination of PhenoCam derived images, satellite derived data or the field observation to study the timing of phenological events (Khare et al. 2019; Khare et al. 2022; Kumar et al. 2025; Li et al. 2023). These methods allow us to reduce the error obtained from satellite that do not pass over the same point each day and may also fill the observation gap obtained during the ground observation. Thus, the PhenoCam tool can be considered as a reliable and accurate tool to study the phenological changes in the tree.

Studies have used the different PhenoCam indices, such as green chromatic coordinate (GCC), red chromatic index (RCC) and excess green index (ExG), to study the canopy greenness and compare with the field and satellite derived data.

In deciduous broadleaf species, GCC is mostly applied to extract the phenological events in trees (Jiang et al. 2022; Richardson et al. 2018). Furthermore, the highest value of RCC corresponded with the timings of autumnal senescence in temperate deciduous forest suggesting being a reliable indicator of autumn phenology (Xie et al. 2018). This study evaluates the effectiveness of three color indices derived from PhenoCam imagery (GCC, ExG, and RCC) in capturing the phenological patterns of sugar maple (*Acer saccharum* Marsh.) using ground-based observations. We tested the hypothesis that GCC exhibits the best performance in representing the onset of leaf color change whereas RCC is suitable for detecting the timing of leaf fall.

2.3 Materials and Methods

2.3.1 Study site

This study was conducted at a site of Centre ACER (L'Assomption; 45.805950° N and 73.467621° W), Quebec, Canada. It is a naturally maple-dominated mixed northern hardwoods forest with sugar maple and silver maple making up 70% of the stems. The forest has been thinned recently to salvage ash trees that were dying from the emerald ash borer but has otherwise not seen little management interventions in the past 100 years. The site is surrounded by a mix of forest and arable land.

2.3.2 Near-Surface Remote Sensing Data

A digital camera FLEX trail camera (SPYPOINT, Quebec, Canada) was installed at 8 m from the ground ensuring the clear coverage of tree canopy. The installed camera was pointed north to avoid shadows and lens flare. To minimize the variability due to scene illumination, automatic white color balance was turned off, and exposure adjustment was set to automatic mode (Richardson et al. 2009, 2007). Images of the canopy were collected every hour and stored in a memory card into the camera. The camera was installed on the study site throughout the study period.

2.3.3 Ground observations

We monitored the leaf phenology of 31 mature sugar maple trees twice a week from early September to early December 2023. For each individual tree, we visually estimated and recorded the percentage of the leaf color change and leaf fall.

These estimates ranged from 0% to 100% until the canopy fully changed the color and all the leaves had fallen off the tree. To characterize the overall trends at the stand level, we calculated averages across all 31 trees for each observation date.

2.3.4 Data extraction

We chose one best image per day between 8 AM to 4 PM to ensure a constant period of image recording. Data was extracted from each image defining eight regions of interest (ROIs) from the areas containing dense leaves of the trees also observed from the ground. The surrounding areas with disturbances such as sky and ground were carefully checked and excluded from data collection. All the indices were extracted from all the ROIs and averaged for each image. We used xROI R package to extract the indexes from the images (Seyednasrollah et al. 2019). Following the data extraction protocol in Richardson et al. (2018), the 90th percentile of phenocam chromatic coordinates across 1-day moving window was calculated.

We extracted three phenocam indices, i.e., red chromatic coordinate (RCC), green chromatic coordinate (GCC), and Excess Green Index (ExG) from different ROIs from the studied period based on the following equations:

$$\boldsymbol{RCC} = \frac{\boldsymbol{DN(Red)}}{\boldsymbol{DN\ (Red) + DN\ (Green) + DN\ (Blue)}}$$

$$\boldsymbol{GCC} = \frac{\boldsymbol{DN(Green)}}{\boldsymbol{DN\ (Red) + DN\ (Green) + DN\ (Blue)}}$$

$$\boldsymbol{ExG} = \boldsymbol{2DN(Green) - (DN(Red) + DN(Blue))}$$

where DN(Red), DN(Green), and DN(Blue) are the red, green, and blue color channels of the phenocam digital camera, respectively, representing digital numbers (DN) saved in JPEG format (Sonnentag et al. 2012). The three channel's combined pixel values were compared to each distinct color band using chromatic coordinate index. RCC was computed to quantify canopy coloring and GCC to quantify canopy greenness, commonly used to identify the seasonal change in phenological phases and canopy development (Klosterman et al. 2014). ExG index is intended as a measurement of greenness for the entire image.

2.3.5 Data Analysis

We applied breakpoint analysis in the field observation data, GCC, and ExG to detect the onset of leaf color change and leaf fall. The two breakpoints given by the model were considered as the onset of leaf senescence and leaf fall respectively.

RCC was fitted using a local regression smoothing method using weighted polynomial regression to produce a stable seasonal signal. This method is implemented in evergreen conifers and minimizes noise filling the gaps along the dataset (Liu et al., 2020). RCC is closely related to anthocyanin and xanthophyll pigments which remain in the tree even after the chlorophyll degradation in autumn (Yang et al. 2014). Relying on this, we extracted the day with lowest and highest value of RCC to find out the day of onset of leaf color change and leaf fall.

To evaluate the relationship between the observed phenological phases and phenocam indices, we calculated root mean square error (RMSE) between the dates estimated from each index and corresponding dates recorded in the field. RMSE

was chosen as it quantifies the average deviation between the predicted and observed values, with lower values indicating stronger agreement.

2.4 Results

2.4.1 Observed leaf phenology

We observed a gradual progression of leaf color change and leaf fall throughout the study period. We extracted two breakpoints for field observations and two breakpoints for phenocam data. The results of field observation showed that the initial color change in the canopy started on DOY 266 with approximately three percent change in canopy color (Fig. 2.1). The canopy turned completely yellow by DOY 294. We observed the first leaf fall on DOY 273 whereas the complete leaf fall was observed on DOY 301.

The segmented model detected the onset of leaf color change on DOY 270 and the complete color change on DOY 290. The model detected the onset of leaf fall on DOY 279 whereas complete leaf fall happened on DOY 292 (Fig. 2.1). Overall, the time between leaf color change and leaf fall lasted about three weeks.

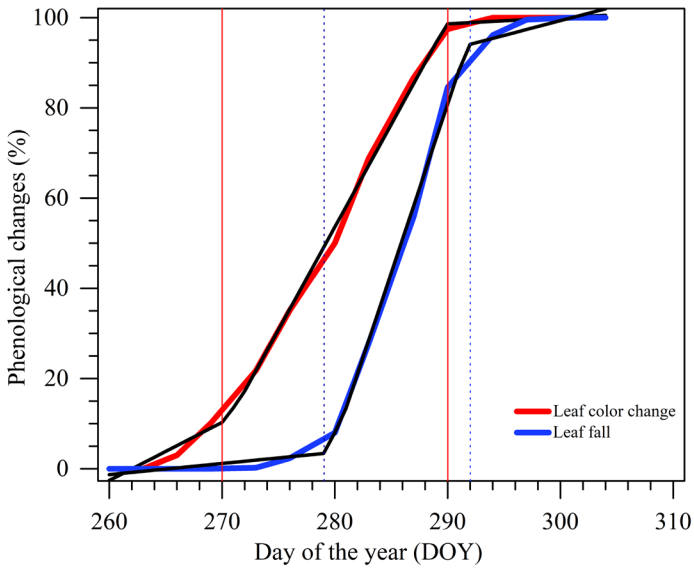

Fig 2.1. Timing of autumn leaf phenological phases for ground observations. The red and blue curves represent the observed leaf color change and leaf fall, respectively whereas the black curves are the fitted segmented model. The vertical lines represent the onset and ending of leaf color change and leaf fall with their respective colors.

2.4.2 Phenocam color indices

GCC showed a decreasing pattern throughout autumn and remained stable after a certain time (Fig. 2.2). Based on the fitted model and the breakpoints extracted, the onset of leaf color change was detected on DOY 270.35 whereas leaf fall occurred on DOY 300 (Fig. 2.2). The value of GCC ranged from 0.44 to 0.33. ExG showed a similar pattern to GCC with the onset of leaf senescence observed on DOY 270.45 and the leaf fall on DOY 298.0 (Fig. 2.2).

RCC represented the autumnal change in leaf phenology. The curve started increasing from the end of September, reaching its peak in late October, which again

decreased quickly reaching the minimum value in winter. We observed the lowest value of RCC on DOY 271 (0.35) whereas the highest value was recorded on DOY 297 (0.42) (Fig. 2.2).

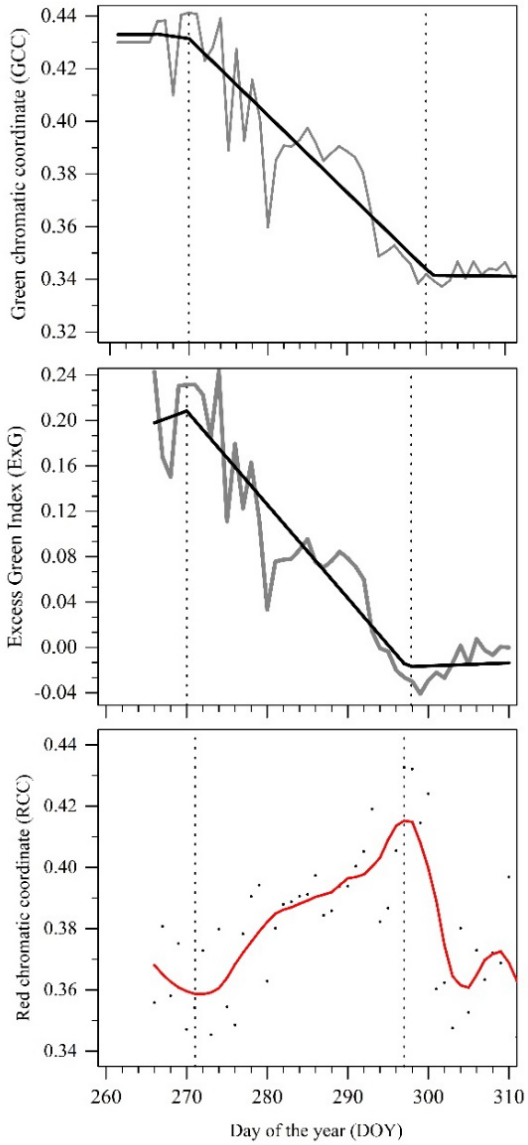

Fig 2.2 Average daily values of GCC and ExG fitted by the segmented model and RCC index smoothed by local regression during the study period. The first and second dotted vertical lines indicate the onset of leaf color change and leaf fall respectively.

Based on RMSE values, both GCC and ExG accurately detected the onset of leaf color change with RMSE values of 0.35 and 0.45 day respectively. RCC differed from the field observation by one day. For the timing of leaf fall, RCC showed the closest agreement with field data (5 days), followed by ExG (6 days) and GCC, which overestimated the date by 8 days. These results suggest that RCC better captured the timing of leaf fall events compared to the other indices

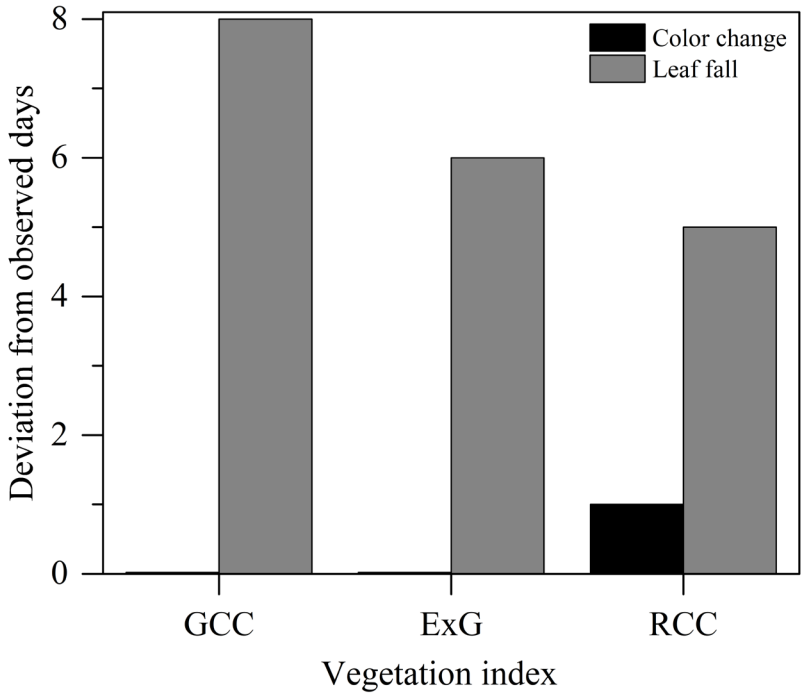

Figure 2.3 Deviation from observed days for each vegetation index (GCC, ExG, RCC) for onset of leaf color change and timing of leaf fall. Low values indicate a better agreement with field observations.

2.5 Discussion

We used ground observations and phenocam imagery to identify the timing of leaf senescence and leaf fall in sugar maple trees in Quebec Canada during the autumn 2023. Our comparison between phenocam derived dates and field-based observation highlights the potential of digital imagery to reliably capture autumn leaf phenology in relation to ground-based methods. The results of digital cameras provided similar patterns of canopy changes as ground observations, but with slightly different metrics for leaf senescence and leaf fall. Our results confirmed that the onset of leaf senescence was comparable with GCC and ExG. Whereas the timing of leaf fall was better explained by RCC. The observed results partially confirmed our initial hypothesis of GCC being a reliable indicator of autumn phenology.

GCC and ExG showed better agreement in capturing the onset of leaf color change in autumn. Recent studies have shown that greenness-based indices such as GCC can reflect seasonal changes in canopy chlorophyll content and leaf pigmentation (Seyednasrollah et al. 2021). Because both GCC and ExG are greenness-based indices, they can effectively capture the decline in chlorophyll before the substantial color change occurs (Xie et al. 2018). At the initial stage of leaf color change, the canopy's overall greenness remains high, allowing these indices to capture the initial physiological changes. However, as the senescence progresses and leaves change from green to yellow or red, greenness-based indices no longer capture substantial changes because the chlorophyll-related signal they rely on start to decrease (Xie et al. 2018). This likely explains the discrepancy between the two greenness indices and field observations for the timing of leaf fall.

As the proportion of green pigments in the canopy diminishes, GCC and ExG remain limited to their ability to reflect the increasing dominance of non-green colors and the eventual loss of foliage. Therefore, while GCC and ExG are useful for detecting the onset of color change, these indices are less reliable for capturing the later stages of autumn phenology, particularly leaf abscission.

RCC showed greater agreement on the timing of leaf fall relative to field observations. During the degradation of chlorophylls, the colors of the pigments such as carotenoids emerge, gradually turning the leaves red and yellow. This color change results in RCC values increasing gradually during the period of senescence. The peak of RCC during autumn has been reported in several studies (Richardson et al. 2009; Xie et al. 2018; Li et al. 2023). The biochemical analysis done during the autumn has shown the close relationship between the peak in RCC and the increase in anthocyanin reflectance index (Yang et al. 2014). The highest value of RCC during the end of October in our study could be related to the highest value of anthocyanin pigment in the leaves. Our finding supports the significance of the use of RCC for detecting the onset of pigment driven color changes in autumn and leaf fall, highlighting its potential to track the later stages of leaf senescence in sugar maple trees.

While visual observations are sensitive to early signs of phenological transition across the crown, they can be subjective and vary between the observers. However, camera-derived indices provide consistent monitoring over time and may pose limited bias. Hence, digital imagery along with ground observations may

provide a promising way to detect autumn leaf phenology in the species like maples that (Xie et al. 2018).

2.6 Conclusion

This study evaluated the effectiveness of phenocams in monitoring autumn leaf phenology of sugar maple with respect to field observations. Our results show that GCC and ExG are best suited for detecting the onset of leaf color change, while RCC more accurately captures both the start and end of leaf fall. These findings demonstrate the reliability of phenocam imagery as a low effort and low-cost alternative to traditional field-based phenological monitoring. Such an approach is useful for planning phenological observations in remote or large areas and in regions with extreme weather conditions where regular human observation is not possible. Monitoring of tree canopy using digital cameras can be easily and economically integrated in further research to monitor various spatial and temporal data on leaf phenology. Further studies incorporating the leaf color change with the amount of chlorophyll degradation through leaf biochemical analysis and assessments of resource relocation could help understand the physiological process underlying autumn senescence.

GENERAL CONCLUSION

This study provides insights into the temporal dynamics and interrelationships among key ph b enological events and evaluates the reliability of phenocameras in comparison with ground-based observations in sugar maple in Quebec, Canada. We observed a clear and consistent order of phenological events during our study of five years indicating a species-specific developmental priority in sugar maple. Sugar season was the first event to occur at the end of March. It occurred while freeze thaw cycles and snow cover were present. Once the snow cover disappeared and both soil and air temperatures began to rise, sap exudation ceased. More importantly, the sugar season ended with the onset of tension driven water transport. The synchronism between the onset of tension driven water transport and pressure driven sap flow suggests the biological limit of sap production. The extraction should be optimized only within the period of sugar season.

The thesis also evaluated the reliability of digital repeat photography for monitoring autumn phenology in sugar maple. By comparing the phenocam derived indices with the field observations, we showed that greenness-based index (GCC) was the best indicator of detecting the onset of autumn leaf color change. Whereas the redness-based index, RCC showed suitability for the timing of leaf fall. These findings confirm that the phenocams are practical and cost-effective alternatives to traditional field-based observations, particularly for continuous monitoring in remote areas.

Together, the two chapters show how understanding both the biological sequence of phenophases and the tools used to monitor them can improve phenological research and maple syrup management. The integration of field observations, dendrometer data, and automated phenocam imaging provides a clear view of how seasonal processes unfold. Future work should expand to more sites across the species range, and link phenology with internal processes such as carbon use and storage.

References

Agriculture and Agri-Food Canada. 2025. Statistical overview of the Canadian maple industry 2024. Horticulture Section, Crops and Horticulture Division. https://agriculture.canada.ca/sites/default/files/documents/2025-03/MapleReport_2024-eng.pdf (accessed on 28 May 2025).

Ahmed S, Lutz D, Rapp J, Huish R, Dufour B, Brunelle A, Morelli TL, Stinson K et Warne T. 2023. Climate change and maple syrup: producer observations, perceptions, knowledge, and adaptation strategies. Frontiers in Forests and Global Change, 6 : 1092218.

Antonucci , Rossi S, Deslauriers A, Lombardi F, Marchetti M et Tognetti R. 2015. Synchronisms and correlations of spring phenology between apical and lateral meristems in two boreal conifers. Tree Physiology, 35 : 1086-1094.

Basler D, et Körner C. 2014. Photoperiod and temperature responses of bud swelling and bud burst in four temperate forest tree species. Tree Physiology, 34 : 377-388.

Beikircher B, Mittmann C et Mayr S. 2016. Prolonged soil frost affects hydraulics and phenology of apple trees. Frontiers in Plant Science, *7*: 867.

Boakye EA, Bergeron Y, Drobyshev I, Beekharry A, Voyer D, Achim A, Huang J. G, Grondin P, Bédard S, Havreljuk F, Gennaretti F et Girardin MP. (2023). Recent decline in sugar maple (*Acer saccharum* Marsh.) growth extends to the northern parts of its distribution range in eastern Canada. Forest Ecology and Management, *545 :* 121304.

Bouchard É, Houle D, Deslauriers A, Jutras S et Messier C. 2025. Unraveling water pathways and sources in leafless maples during early spring sap ascent. New Phytologist, 247 : 3.

Brodersen CR, et McElrone AJ. 2013. Maintenance of xylem network transport capacity: a review of embolism repair in vascular plants. Frontiers in Plant Science, 4 : 108.

Buttò V, Khare S, Jain P, de Lima Santos G et Rossi S. 2023. Spatial patterns and climatic drivers of leaf spring phenology of maple in eastern North America. Science of Total Environment, 857 : 159064.

Christensen Dalsgaard KK et Tyree M. T. 2014. Frost fatigue and spring recovery of xylem vessels in three diffuse-porous trees in situ. Plant, Cell Environment, 37 : 1074-1085.

Cochard H, Lemoine D, Améglio T et Granier A. 2001. Mechanisms of xylem recovery from winter embolism in *Fagus sylvatica*. Tree Physiology, 21 : 27-33.

Croft H, Chen JM et Zhang Y. 2014. Temporal disparity in leaf chlorophyll content and leaf area index across a growing season in a temperate deciduous forest. International Journal Applied Earth Observation and Geoinformation, 33 : 312-320.

Čufar K, Prislan P, de Luis M et Gričar J. 2008. Tree-ring variation, wood formation and phenology of beech (*Fagus sylvatica*) from a representative site in Slovenia, SE Central Europe. Trees, 22 : 749-758.

Cuny HE, Rathgeber CB, Frank D, Fonti P, Mäkinen H, Prislan P, Fournier M. et al. 2015. Woody biomass production lags stem-girth increase by over one month in coniferous forests. Nature Plants, 1 : 1-6.

de Lima Santos G, Silvestro R, Kurokawa SYS, De Lafontaine G et Rossi S. 2025. Reassessing the schedule of the sugar season in maple under climate warming. Frontiers in Agronomy, 6 : 1-11.

Deslauriers A, Giovannelli , Rossi S, Castro G, Fragnelli G et Traversi L. 2009. Intra-annual cambial activity and carbon availability in stem of poplar. Tree Physiology, 29 : 1223-1235.

D'Orangeville L, Itter M, Kneeshaw D, Munger JW, Richardson AD, Dyer JM, Orwig DA, Pan Y et Pederson N. 2022. Peak radial growth of diffuse-porous species occurs during periods of lower water availability than for ring-porous and coniferous trees. Tree Physiology, 42 : 304-316.

Dox I, Gričar J, Marchand LJ, Leys S, Zuccarini P, Geron C, Prislan P, Mariën B, Fonti P, Lange H, Peñuelas J, van den Bulcke J et Campioli M. 2020. Timeline of autumn phenology in temperate deciduous trees. Tree Physiology, 40 : 1001-1013.

Eglin T, Fresneau C, Lelarge Trouverie C, Francois C et Damesin C. 2009. Leaf and twig δ13C during growth in relation to biochemical composition and respired CO2. Tree Physiology, 29 : 777-788.

Essiamah S et Eschrich W. 1986. Water uptake in deciduous trees during winter and the role of conducting tissues in spring reactivation. IAWA, 7 : 31-38.

Ettinger AK, Gee S et Wolkovich EM. 2018. Phenological sequences: how early-season events define those that follow. American Journal of Botany, *105 :* 1771-1780.

Fracheboud Y, Luquez V, Bjorken L, Sjodin A, Tuominen H et Jansson S. 2009. The control of autumn senescence in European aspen. Plant physiology, 149 : 1982-1991.

Graf I, Ceseri M, et Stockie JM. 2015. Multiscale model of a freeze-thaw process for tree sap exudation. Journal of the Royal Society Interface, 12 : 20150665.

Gray REJ et Ewers RM. 2021. Monitoring forest phenology in a changing world. Forests, 12 : 297.

Gao J, Mura C, Kurokawa SYS, Silvestro R, Rademacher T, Delagrange S, Fang K, Yang B et Rossi S. 2025. Warmer springs advance bud phenology in sugar maple at its northern range limits in Canada. Journal of Forestry Research, 36.

Guo X, Khare S, Silvestro R, Huang J, Sylvain J. D, Delagrange S et Rossi S. 2020. Minimum spring temperatures at the provenance origin drive leaf phenology in sugar maple populations. Tree Physiology, 40 : 1639-1647.

Hölttä T, Dominguez Carrasco MDR, Salmon Y, Aalto J, Vanhatalo A, Bäck J et Lintunen A. 2018. Water relations in silver birch during springtime: How is sap pressurised?. Plant Biology, 20 : 834-847.

Jiang N, Shen M, Ciais P, Campioli M, Peñuelas J, Körner C, Cao R, Piao S, Liu L, Wang S, Liang E, Delpierre, N, Soudani K, Rao Y, Montagnani L, Hörtnagl L, Paul-Limoges E, Myneni R, Wohlfahrt G, Fu Y, Šigut L, Varlagin A, Chen J, Tang Y et Zhao W. 2022. Warming does not delay the start of autumnal leaf coloration but slows its progress rate. Global Ecology and Biogeography, 31 : 2049–2062.

Keskitalo J, Bergquist G, Gardeström P et Jansson S. 2005. A cellular timetable of autumn senescence. Plant Physiology, 139 : 1635-1648.

Khare S, Deslauriers A, Morin H, Latifi H et Rossi S. 2021. Comparing time-lapse PhenoCams with satellite observations across the boreal forest of Quebec, Canada. Remote Sensing, 14 : 100.

Khare S, Drolet G, Sylvain JD, Paré MC et Rossi S. 2019. Assessment of spatio-temporal patterns of black spruce bud phenology across Quebec based on MODIS-NDVI time series and field observations. Remote Sensing, 11 : 2745.

Klein T, Vitasse Y et Hoch G. 2016. Coordination between growth, phenology and carbon storage in three coexisting deciduous tree species in a temperate forest. Tree physiology, 36 : 847-855.

Klosterman ST, Hufkens Ks, Gray JM, Melaas E, Sonnentag O, Lavine I, Mitchell L, Norman R, Friedl MA et Richardson AD. 2014. Evaluating remote sensing of deciduous forest phenology at multiple spatial scales using PhenoCam imagery. Biogeosciences, 11 : 4305–4320.

Kudo K, Yasue K, Hosoo Y et Funada R. 2015. Relationship between formation of earlywood vessels and leaf phenology in two ring-porous hardwoods, *Quercus*

serrata and *Robinia pseudoacacia*, in early spring. Journal of Wood Science, 61 : 455-464.

Kumar A, Noolu GSS, Khare S et Rossi S. 2025. A comparison of PhenoCam and satellite indices with in-situ observations for black spruce in the boreal forest of Quebec, Canada. Ecological Informatics, 88 : 103137.

Kurokawa SYS, Silvestro R, Khan A, de Lima Santos G, Delagrange S et Rossi S. 2025. The divergent advancements of sap phenology in maple under warming conditions can shorten the sugar season. Trees, Forests and People, 19 : 100779.

Kurokawa SYS, Weiss G, Lapointe D, Delagrange S et Rossi S. 2022. Daily timings of sap production in sugar maple in Quebec, Canada. International Journal of Biometeorology, 67 : 211-218.

Lavrič M, Eler K, Ferlan M, Vodnik D et Gričar J. 2017. Chronological sequence of leaf phenology, xylem and phloem formation and sap flow of *Quercus pubescens* from abandoned karst grasslands. Frontiers in Plant Science, 8 : 314.

Li X, Khare S, Khare S, Jiang N, Liang E, Deslauriers A et Rossi S. 2023. Comparing phenocam color indices with phenological observations of black spruce in the boreal forest. Ecological Informatics, 76 : 102149.

Liu Y, Wu C, Sonnentag O, Desai AR et Wang J. 2020. Using the red chromatic coordinate to characterize the phenology of forest canopy photosynthesis. Agriculture and Forest Meteorology, 285-286 : 107910.

Melcher PJ, Zwieniecki MA et Holbrook NM. 2003. Vulnerability of xylem vessels to cavitation in sugar maple. Scaling from individual vessels to whole branches. Plant Physiology, 131 : 1775-1780.

Michelot A, Simard S, Rathgeber C, Dufrêne E et Damesin C. 2012. Comparing the intra-annual wood formation of three European species *(Fagus sylvatica, Quercus petraea and Pinus sylvestris*) as related to leaf phenology and non-structural carbohydrate dynamics. Tree physiology, 32 : 1033-1045.

Mura C, Charrier G, Buttò V, Delagrange S, Surget Groba Y, Raymond P, Rossi S et Deslauriers A. 2025. Local conditions have greater influence than provenance on sugar maple (*Acer saccharum* Marsh.) frost hardiness at its northern range limit. Tree Physiology, 45.

N'guyen GQ, Martin N, Jain M, Lagacé L, Landry CR et Filteau M. 2018. A systems biology approach to explore the impact of maple tree dormancy release on sap variation and maple syrup quality. Scientific Reports, 8 : 14658.

Nehemy MF, Maillet J, Perron N, Pappas C, Sonnentag O, Baltzer JL, Laroque CP et McDonnell JJ. 2022. Snowmelt water use at transpiration onset: Phenology,

isotope tracing, and tree water transit time. Water Resources Research, 58 : e2022WR032344.

Niu CY, Meinzer FC et Hao GY. 2017. Divergence in strategies for coping with winter embolism among co-occurring temperate tree species: the role of positive xylem pressure, wood type and tree stature. Functional Ecology, 31 : 1550-1560.

Park J et Post E. 2022. Phenological evolution on a cyclical Earth: towards first principles and null expectations. Author Preprints.

Pasqualotto G, Ascari L, Bicego G, Carraro V, Huerta ES, De Gregorio T, Siniscalco C et Anfodillo T. 2022. Radial stem growth dynamics and phenology of a multi-stemmed species (*Corylus avellana* L.) across orchards in the Northern and Southern hemispheres. Tree Physiology, 41: 2022-2033.

Perkins TD, Heiligmann RB, Koelling MR et van den Berg AK. 2022. North American maple syrup producers manual. North American Maple Syrup Council, 434 p.

Prislan P, Gričar J, de Luis M, Smith KT et Čufar K. 2013. Phenological variation in xylem and phloem formation in *Fagus sylvatica* from two contrasting sites. Agriculture and Forest Meteorology, 180 : 142-151.

Ramadan MF, Gad HA et Farag MA. 2021. Chemistry, processing, and functionality of maple food products: An updated comprehensive review. Journal of Food Biochemistry, 45 : e13832-e13832.

Rapp JM, Lutz DA, Huish RD, Dufour B, Ahmed S, Morelli TL et Stinson KA. 2019. Finding the sweet spot: Shifting optimal climate for maple syrup production in North America. Forest Ecology and Management, 448 : 187-197.

Richardson AD, Bailey AS, Denny EG, Martin CW et O'Keefe J. 2006. Phenology of a northern hardwood forest canopy. Global Change Biology, 12 : 1174-1188.

Richardson AD, Braswell BH, Hollinger DY, Jenkins JP et Ollinger SV. 2009. Near-surface remote sensing of spatial and temporal variation in canopy phenology. Ecological Applications, 19 : 1417–1428.

Richardson AD, Hufkens K, Milliman T, Aubrecht DM, Chen M, Gray JM, Johnston MR, Keenan TF, Klosterman ST, Kosmala M, Melaas EK, Friedl MA et Frolking S. 2018. Tracking vegetation phenology across diverse north American biomes using PhenoCam imagery. Scientific Data, 5 : 180028.

Robitaille G, Boutin R et Lachance D. 1995. Effects of soil freezing stress on sap flow and sugar content of mature sugar maples (*Acer saccharum*). Canadian Journal of Forest Research, 25 : 577-587.

Rossi S, Rathgeber CB et Deslauriers A. 2009. Comparing needle and shoot

phenology with xylem development on three conifer species in Italy. Annals of Forest Sciences, 66 : 1-8.

Rossi S, Morin H et Deslauriers A. 2011. Multi-scale influence of snowmelt on xylogenesis of black spruce. Arctic Antarctic and Alpine Research, 43 : 457-464.

Rossi S, Morin H et Deslauriers A. 2012. Causes and correlations in cambium phenology: towards an integrated framework of xylogenesis. Journal of Experimental Botany, 63 : 2117-2126.

Salleo S, Nardini A, Lo Gullo MA et Ghirardelli LA. 2002. Changes in stem and leaf hydraulics preceding leaf shedding in *Castanea sativa* L. Biologia plantarum, 45 : 227-234.

Seyednasrollah B, Bowling DR, Cheng R, Logan BA, Magney TS, Frankenberg C, Yang JC, Young AM, Hufkens K, Arain MA, Black TA, Blanken PD, Bracho R, Jassal R, Hollinger DY, Law BE, Nesic Z et Richardson AD. 2021. Seasonal variation in the canopy color of temperate evergreen conifer forests. New Phytologist, 229 : 2586–2600.

Seyednasrollah B, Milliman T et Richardson AD. 2019. Data extraction from digital repeat photography using xROI: an interactive framework to facilitate the process. ISPRS Journal of Photogrammetry and Remote Sensing, 152 : 132–144.

Silvestro R, Deslauriers A, Prislan P, Rademacher T, Rezaie N, Richardson AD, Vitasse Y, et Rossi S. 2025. From Roots to Leaves: Tree Growth Phenology in Forest Ecosystems. Current Forest Reports, 11 : 1-19.

Silvestro R, Mencuccini M, García Valdés R, Antonucci S, Arzac A, Biondi F et al. 2024. Partial asynchrony of coniferous forest carbon sources and sinks at the intra-annual time scale. Nature Communications, 15 : 6169.

Sonnentag O, Hufkens K, Teshera Sterne C, Young AM, Friedl M, Braswell BH, Milliman T, O'Keefe J et Richardson A. 2012. Digital repeat photography for phenological research in forest ecosystems. Agriculture and Forest Meteorology, 152 : 159–177.

Sperry JS, Donnell, JR et Tyree MT. 1988. Seasonal occurrence of xylem embolism in sugar maple (*Acer saccharum*). American Journal of Botany, 75 : 1212-1218.

Sperry JS, Nichols KL, Sullivan JE et Eastlack SE. 1994. Xylem embolism in ring-porous, diffuse-porous, and coniferous trees of northern Utah and interior Alaska. Ecology, 75 : 1736-1752.

Suzuki M, Yoda K, et Suzuki H. 1996. Phenological comparison of the onset of vessel formation between ring-porous and diffuse-porous deciduous trees in a Japanese temperate forest. IAWA Journal, 17 : 431-444.

Turcotte A, Morin H, Krause C, Deslauriers A et Thibeault Martel M. 2009. The timing of spring rehydration and its relation with the onset of wood formation in black spruce. Agriculture and Forest Meteorology, 149 : 1403-1409.

Tyree MT et Cochard H. 1996. Summer and winter embolism in oak: impact on water relations. In Annales des sciences forestières, 53 : 173-180.

Utsumi Y, Sano Y, Fujikawa S, Funada R et Ohtani J. 1998. Visualization of cavitated vessels in winter and refilled vessels in spring in diffuse-porous trees by cryo-scanning electron microscopy. Plant Physiology, 117 : 1463-1471.

Wang H, Wu C, Ciais P, Peñuelas J, Dai J, Fu Y et Ge Q. 2020. Overestimation of the effect of climatic warming on spring phenology due to misrepresentation of chilling. Nature Communications, 11 : 4945.

White MA, de Beurs KM, Didan K, Inouye DW, Richardson AD, Jensen OP, Lauenroth WK et al. 2009. Intercomparison, interpretation, and assessment of spring phenology in North America estimated from remote sensing for 1982-2006. Global Change Biology, 15 : 613-615.

Xie Y, Wang X, Wilson AM et Silander JrJA. 2018. Predicting autumn phenology: How deciduous tree species respond to weather stressors. Agricultural and Forest Meteorology, 250 : 127-137.

Yang X, Tang J et Mustard JF. 2014. Beyond leaf color: comparing camera-based phenological metrics with leaf biochemical, biophysical, and spectral properties throughout the growing season of a temperate deciduous forest. Journal of Geophysical Research: Biogeosciences, 119 : 181–191.

Zhang S, Buttò V, Khare S, Deslauriers A, Morin H, Huang JG, Ren H et Rossi S. 2020. Calibrating PhenoCam data with phenological observations of a black spruce. Canadian Journal of Remote Sensing. 46 : 154–165.

Zhang X, Friedl MA, Schaaf C. B, Strahler AH, Hodges JCF, Gao F, Reed BC et Huete A. 2003. Monitoring vegetation phenology using MODIS. Remote sensing of environment, 84 : 471-475.

Zweifel R, Zimmermann L, Zeugin F et Newbery DM. 2006. Intra-annual radial growth and water relations of trees: implications towards a growth mechanism. Journal of Experimental Botany, 57 : 1445-1459.